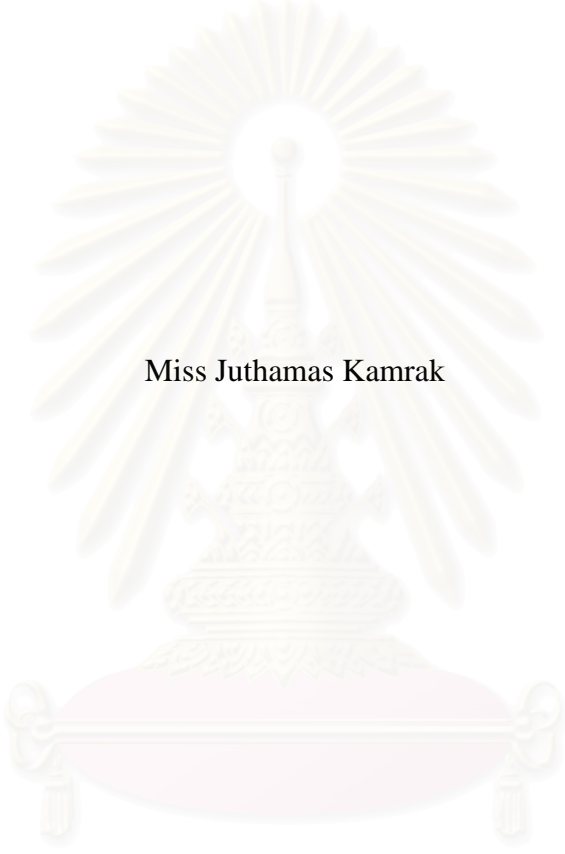


CHARACTERIZATION OF MIXTURE OF PALM OIL AND DIESEL ATOMIZED BY
A TWO-FLUID NOZZLE USING PHASE DOPPLER ANEMOMETER



Miss Juthamas Kamrak

สถาบันวิทยบริการ
A Thesis Submitted in Partial Fulfillment of the Requirements
for the Degree of Master of Engineering Program in Chemical Engineering

Department of Chemical Engineering

Faculty of Engineering, Chulalongkorn University

Academic Year 2006

Copyright of Chulalongkorn University

การศึกษาคุณลักษณะของของผสมจากน้ำมันปาล์มและดีเซลที่ทำให้เป็นละอองด้วยหัวฉีดชนิดทูลูอิด
โดยใช้เครื่องมือเฟสคอปเพลอร์อิมมิเตอร์



นางสาว จุฑามาศ คามรัมย์

สถาบันวิทยบริการ

จุฬาลงกรณ์มหาวิทยาลัย

วิทยานิพนธ์นี้เป็นส่วนหนึ่งของการศึกษาตามหลักสูตรปริญญาวิศวกรรมศาสตรมหาบัณฑิต

สาขาวิชาวิศวกรรมเคมี ภาควิชาวิศวกรรมเคมี

คณะวิศวกรรมศาสตร์ จุฬาลงกรณ์มหาวิทยาลัย

ปีการศึกษา 2549

ลิขสิทธิ์ของจุฬาลงกรณ์มหาวิทยาลัย

จุฬามาศ ความรักษ์ : การศึกษาคุณลักษณะของของผสมจากน้ำมันปาล์มและดีเซลที่ทำให้
เป็นละอองด้วยหัวฉีดชนิดทูลูฟลูอิดโดยใช้เครื่องมือเฟสคอปเปิลเลอร์อนิโมมิเตอร์

(CHARACTERIZATION OF MIXTURE OF PALM OIL AND DIESEL ATOMIZED
BY A TWO-FLUID NOZZLE USING PHASE DOPPLER ANEMOMETER)

อ. ที่ปรึกษา : รศ.ดร.ธวัชชัย ชรินพณิชกุล, 98 หน้า.

จากวิกฤตการณ์น้ำมันที่เกิดขึ้นไม่ว่าจะเป็นภาวะราคาเชื้อเพลิงที่สูงขึ้นและปริมาณเชื้อเพลิงสำรอง
ที่ลดลงอีกทั้งความต้องการที่มีแนวโน้มเพิ่มมากขึ้นอย่างต่อเนื่อง ดังนั้นจึงมีการพยายามหาเชื้อเพลิง
ทดแทนมาใช้แทนเชื้อเพลิงจากแหล่งปิโตรเลียม โดยที่น้ำมันไบโอดีเซลที่ได้จากพืชน้ำมันต่างๆ รวมทั้ง
เชื้อเพลิงจากพืชน้ำมันโดยตรงเป็นตัวเลือกที่กำลังได้รับความสนใจอย่างมาก หากแต่ยังไม่มีการทำการ
ทดลองเพื่อหาคุณลักษณะของสเปรย์จากเชื้อเพลิงเหลวดังกล่าว คุณลักษณะที่กล่าวถึงคือ ขนาดและ
ความเร็วของหยดที่เกิดจากการสเปรย์จากหัวฉีด ข้อมูลที่ได้มาดังกล่าวนี้มีความสำคัญต่อการนำไปศึกษา
ทางด้าน การเผาไหม้ของหยดเชื้อเพลิง เพื่อสามารถควบคุมและกำหนดการระเหยของหยด ค่าความร้อนที่
ได้จากการเผาไหม้ เพื่อการเผาไหม้ที่มีประสิทธิภาพ ลดมลภาวะจากอนุภาคและสารจากการเผาไหม้

งานนี้ทำการศึกษาหาค่าขนาดและความเร็ว ของหยดละอองน้ำมันดีเซล และน้ำมันผสม ระหว่าง
น้ำมันดีเซลและน้ำมันปาล์ม โดยใช้เฟสคอปเปิลเลอร์อนิโมมิเตอร์ ซึ่งใช้หลักการการกระเจิงของแสงเมื่อมี
อนุภาควิ่งผ่าน ความเร็วของอนุภาคสามารถหาได้จากค่าความถี่ของแสงที่กระเจิง และขนาดของอนุภาคมา
จากข้อมูลของเฟสของแสง สำหรับหัวฉีดที่ใช้ในงานนี้คือ หัวฉีดชนิด two-fluid ซึ่งเป็นหัวฉีดที่มีการใช้
อย่างแพร่หลายในงานด้านการเผาไหม้ โดยมีข้อดีคือสามารถสเปรย์ของเหลวที่มีความหนืดสูงได้ เช่น
เชื้อเพลิงเหลวจากน้ำมันพืชหรือไบโอดีเซล

หัวฉีดชนิดนี้ให้อนุภาคขนาดใหญ่เมื่อใช้อากาศสเปรย์ที่ความดันต่ำ อีกทั้งขนาดของหยดมีการ
เปลี่ยนแปลงตามระยะทางที่หยดของเหลววิ่งผ่าน โดยที่ระยะทางห่างจากหัวฉีดจะพบหยดขนาดใหญ่และ
ความเร็วลดลง อีกทั้งคุณสมบัติของของเหลวมีผลต่อการสเปรย์จากหัวฉีดและการกระจายของขนาด
โดยเฉพาะความหนืดของของเหลว โดยที่ของเหลวที่มีความหนืดสูงส่งผลให้การสเปรย์เกิดได้ยากกว่าและ
หยดมีขนาดใหญ่ หากแต่ไม่ส่งผลต่อความเร็วของหยด ที่ความดันอากาศที่ใช้ในการสเปรย์มีผลมากกว่า

ภาควิชา.....วิศวกรรมเคมี..... ลายมือชื่อนิสิต.....
สาขาวิชา.....วิศวกรรมเคมี..... ลายมือชื่ออาจารย์ที่ปรึกษา.....
ปีการศึกษา.....2549.....

4870259621 : MAJOR CHEMICAL ENGINEERING

KEY WORD: ATOMIZATION / PHASE DOPPLER / TWO-FLUID NOZZLE / VEGETABLE OIL/PARTICLE SIZE DISTRIBUTION

JUTHAMAS KAMRAK : CHARACTERIZATION OF MIXTURE OF PALM OIL AND DIESEL ATOMIZED BY A TWO-FLUID NOZZLE USING PHASE DOPPLER ANEMOMETER. THESIS ADVISOR : ASSOC. PROF. TAWATCHAI CHARINPANITKUL, D. Eng., 98 pp.

Because of the current energy crisis, an increase in fuel price and a decrease in its supply rise an increasing attention of an alternative fuel. Biodiesel is one of the most interesting alternative fuels which can be produced from many plants. Meanwhile drop size and dynamic of its spray has not been investigated clearly yet. Such detailed measurements play an important role in an enhancement of combustion efficiency, it would be employed for optimizing heat transfer, controlling evaporation, and lessening emission.

In order to obtain this initial information, a PDA technique was used to measure the local drop size and velocity of mixture of diesel and palm oil. The method is based on light scattering interferometry. From frequency change, it provides information on droplet velocity while the droplet size is evaluated from the phase change of the laser. The atomizer used in this work is a two-fluid atomizer which has been applied for combustion aid because it can atomize high viscosity liquids like vegetable oil fuel.

It was experimentally observed that the atomizer generates a spray with large drops at low air injection pressure. Large droplets are produced along traveling distance. Therefore, the large drops with low velocity are found at downstream distances far from the nozzle tip. Moreover, the properties of liquid fuel such as viscosity, affect the atomization and the droplet size distribution. Liquids with high viscosity cause poor atomization, resulting in larger drops. However, liquid viscosity could provide only a small effect on the velocity profile if compressed with the air injection pressure.

Department.....Chemical Engineering.....Student's signature.....*Juthamas Kamrak*.....
 Field of study....Chemical Engineering.....Advisor's signature.....*T. Charinpanitkul*.....
 Academic year...2006.....

ACKNOWLEDGEMENTS

First of all, I would like to express my gratitude to my advisor, Associate Professor Tawatchai Charinpanitkul for his encouraging guidance, helpful suggestions and moral support throughout this study. I am also very grateful for the great opportunity he had given me to be an exchange student in France.

I am very thankful to Dr. Gerard Grehan (Director of LESP Laboratory INSA de Rouen, France) for his on-the-job training, advice, helpful suggestions, and all great help while I was in France and also during his visits to Thailand. I have learned a lot of things from him and gained great experiences.

Moreover, I would like to thank Associate Professor Suttichai Assabumrungrat, Assistant Professor Varong Pavaranjarn, Dr. Varun Taepaisitphongse, and Assistant Professor Pумыos Vallikul (from King Mongkut Institute of Technology North Bangkok) for their effort as reviewers and participants on the committee for this thesis.

Likewise, my special thanks go to my colleagues at Complexe de Recherche Interprofessionnel en Aerothemochimie (CORIA), France, for their help when I needed it and for their kindness that lessened my pain while I was far away from family and friends. In addition, thanks to all members of Center of Excellence in Particle Technology (CEPT) for their warm collaboration and kindness. Furthermore, special thanks go to Dr. Sawitree Saengkaew for her support and her talent in stimulating me throughout this work, and Mr. Tanonchai Boonnathee for his kind and useful help with the homemade PDA.

Additionally, I would like to express my appreciation to the Franco-Thai exchange program for supporting my research at CORIA, France, for 8 months (September 2005-April 2006). This research was also partially supported by Department of Chemical Engineering during my study at Chulalongkorn University.

Finally, I wish to express my deepest thanks to my parents, all members in my family and my boyfriend for their love, encouragement and belief in me.

CONTENTS

	Page
ABSTRACT IN THAI	iv
ABSTRACT IN ENGLISH	v
ACKNOWLEDGEMENTS	vi
CONTENTS	vii
LIST OF TABLES	ix
LIST OF FIGURES	x
NOMENCLATURES	xiii
CHAPTER	
1 INTRODUCTION	1
1.1 Purpose and Description.....	1
1.2 Objective.....	2
1.3 Scope of Study.....	2
1.4 Obtained Benefit	3
2 SURVEY OF APPLICATIONS	4
2.1 Applications of Vegetable Oil as Renewable Fuel.....	4
2.2 Applications of Spray Atomization.....	6
2.3 Applications of PDA Technique.....	8
3 EXPERIMENTAL	11
3.1 Experimental Apparatus.....	11
3.2 Fuel Preparation.....	18
3.3 Spray Characterization.....	19
4 ATOMIZATION AND SPRAY	21
4.1 Basic Process in Atomization.....	23
4.2 Drop Size Distribution and Sprays.....	25
4.2.1 Graphical Representation of Drop Size Distribution.....	25
4.2.2 Mean Diameters.....	28
4.2.3 Representative Diameters.....	30
4.3 Atomizers.....	30

CHAPTER	Page
4.3.1 Pressure Atomizers.....	31
4.3.2 Rotary Atomizers.....	33
4.3.3 Air-Assist Atomizers.....	33
4.3.4 Airblast Atomizers.....	34
4.3.5 Electrostatic Atomizers.....	35
4.3.6 Ultrasonic Atomizers.....	35
5 MEASUREMENT TECHNIQUES.....	38
5.1 Experimental Methods for Determining Droplet Size Distribution...	38
5.1.1 Mechanical Methods.....	38
5.1.2 Electrical Methods.....	40
5.1.3 Optical Methods.....	40
5.2 Measurement of Droplet Velocity.....	42
5.3 Laser Doppler Velocimetry (LDV).....	43
5.4 Phase Doppler Anemometer (PDA).....	46
6 RESULTS AND DISCUSSION.....	51
6.1 Measurement by the Homemade PDA.....	51
6.2 Stages of Atomization.....	53
6.3 Discharge Coefficient.....	54
6.4 Size and Velocity Measurement by a Commercial PDA.....	56
7 CONCLUSION AND RECOMMENDATION.....	74
7.1 Concluding Remarks.....	74
7.2 Recommendations.....	75
REFERENCES.....	76
APPENDICES.....	79
APPENDIX A BASIC OPTICS.....	80
APPENDIX B CONFERENCE PAPERS.....	91
VITA.....	98

LIST OF TABLES

	Page
Table 2.1 A list of the advantages and disadvantages of the phase Doppler technique.....	9
Table 3.1 The Dantec PDA configurations and parameters.....	16
Table 3.2 The specification of the homemade PDA system.....	17
Table 3.3 The fuels properties.....	18
Table 4.1 Spray applications.....	21
Table 4.2 Mean Diameters and their Applications.....	29
Table 4.3 Summary the types of atomizers.....	36
Table 6.1 Mean velocity of water spray measured by homemade PDA.....	52
Table 6.2 Arithmetic mean diameter of the spray in different measuring points.....	57
Table 6.3 Size distribution parameters of diesel, PO20:D80, and PO50:D50 sprays ($P_{inj} = 1$ bar, $z = 5$ cm, center of spray).....	57
Table 6.4 Axial mean velocities of fuel droplets at the center of the spray.....	73

LIST OF FIGURES

	Page
Figure 3.1 Schematic diagram of spray system.....	11
Figure 3.2 Picture of fuel injection system.....	12
Figure 3.3 Schematic diagram of external mix with siphon set-ups: Round Spray Pattern.....	13
Figure 3.4 Schematic diagram of Spray Set-ups: Each spray set-up consists of an air-cap and fluid cap.....	13
Figure 3.5 XYZ translation system and stand.....	14
Figure 3.6 (a) The commercial PDA (Dantec Ltd.) (b) transmitting part (c) collecting part (d) laser source.....	15
Figure 3.7 Schematic diagram of homemade PDA.....	17
Figure 3.8 Schematic diagram of local drop size measurements.....	20
Figure 4.1 Typical drop size histogram.....	25
Figure 4.2 Drop size histogram.....	26
Figure 4.3 Drop size frequency distribution curve.....	26
Figure 4.4 Cumulative drop size distribution curve.....	27
Figure 4.5 Spray structure produced by Simplex or pressure-swirl atomizer.....	32
Figure 4.6 Internal-mixing air-assist atomizers.....	33
Figure 4.7 External-mixing air-assist atomizers.....	34
Figure 4.8 Prefilming airblast atomizer.....	34
Figure 4.9 Ultrasonic nozzle assembly.....	35
Figure 5.1 Crossing of two laser beams with angle 2α	43
Figure 5.2 Dimensions of LDA probe volume.....	45
Figure 5.3 Typical optical setup of LDA instrument.....	46
Figure 5.4 (a) A scheme of the optical probe with fringes (b) PDA Configuration.....	46
Figure 5.5 The definition of the scattering angle for a standard configuration....	48

	Page
Figure 5.6 Determination of phase shift from two band-pass filtered Doppler signal.....	49
Figure 5.7 Representative response functions for a PDA system using three detectors.....	50
Figure 6.1 Sprays development by an external-mixed two-fluid atomizer.....	53
Figure 6.2 Effect of injection pressure on discharge coefficient of two-fluid atomizer.....	55
Figure 6.3 Effect of volume ratio of palm oil to diesel on discharge coefficients of fuels at 1 bar air injection pressure.....	55
Figure 6.4 Effect of volume ratio of palm oil on Kinematic viscosity of blended fuel.....	56
Figure 6.5 Mean diameter (D_{10}) versus the injection pressure for PO20:D80 spray at 5 cm away from atomizer tip.....	59
Figure 6.6 Droplet size distribution of PO20:D80 spray. The injection pressure is equal to (a) 0.5 bars (b) 1 bar (c) 4 bars.....	60
Figure 6.7 Effect of air injection pressure on span of drop size distribution.....	61
Figure 6.8 Sauter Mean Diameter (D_{32}) versus the injection pressure for PO20:D80 spray at 5 cm.....	61
Figure 6.9 Velocity profile of PO20:D80 on the center region of spray ($z = 5$ cm).....	62
Figure 6.10 The effect of downstream distance on spray for Mean Diameter (D_{10}) (PO20:D80, $P_{inj} = 4$ bar).....	63
Figure 6.11 The effect of downstream distance on spray for Sauter Mean Diameter (D_{32}) (PO20:D80), $P_{inj} = 4$ bar).....	64
Figure 6.12 The effect of downstream distance on spray for Sauter Mean Diameter (D_{32}) (PO50:D50, $P_{inj} = 2$ bar).....	65
Figure 6.13 Drop size distribution of PO20:D80 with 4 bar injection pressure (a) 5 cm away from atomizer tip (b) 7 cm away from atomizer tip.....	66

	Page
Figure 6.14 Mean velocity of drop along traveling distance.....	67
Figure 6.15 Radial distribution of Mean Diameter (D_{10}) at 5 cm away from atomizer tip ($P_{inj} = 1$ bar).....	68
Figure 6.16 Radial distribution of Sauter Mean Diameter (D_{32}) at 5 cm. away from atomizer tip ($P_{inj} = 1$ bar).....	68
Figure 6.17 The velocity profile of spray at 7 cm. away from nozzle tip (Diesel, $P_{inj} = 1$ bar).....	69
Figure 6.18 Parameters of drop size distribution of diesel, PO5:D95, PO10:D90, PO15:D85, PO20:D80, PO50:D50 and palm oil ($P_{inj} = 1$ bar, $z = 5$ cm).....	70
Figure 6.19 Velocity profiles of diesel and the mixtures spray at 5 cm away from tip ($P_{inj} = 1$ bar).....	71
Figure 6.20 Axial mean velocity of PO20:D80 with different injection pressure at 5 cm. away from atomizer tip.....	72
Figure 6.21 Axial mean velocity of PO20:D80 with different injection pressure at 7 cm. away from atomizer tip.....	72

NOMENCLATURES

m_L	=	mass flow rate (kg/s)
ρ_L	=	density of liquid (kg/m ³)
C_d	=	discharge coefficient (-)
d_o	=	diameter of orifice (m)
l_o	=	length of orifice (m)
A_o	=	orifice area (m ²)
p_l	=	internal pressure of drop (N/m ²)
p_A	=	aerodynamic pressure (N/m ²)
p_σ	=	surface tension pressure (N/m ²)
D	=	drop size diameter (μ m)
N_i	=	number of drop in size range i (-)
f_D	=	Doppler frequency (Hz)
f_e	=	frequency of the laser source (emitter) (Hz)
f_r	=	frequency of the scattered light (Hz)
N_f	=	number of fringes (-)
v	=	velocity of the moving particle (m/s)
d_f	=	fringe spacing (μ m)
d_m	=	waist diameter of laser (mm)
n	=	refractive index of substance (-)
T	=	time of one cycle of the signal (sec)
X	=	dimensionless x-coordinate (-)
Y	=	dimensionless y-coordinate (-)
Z	=	dimensionless z-coordinate (-)
z	=	distance along the beam from the cross-section of minimum diameter (mm)
D_{10}	=	arithmetic mean diameter (μ m)
D_{32}	=	Sauter mean diameter (μ m)
$D_{0.1}$	=	drop diameter such that 10% of total liquid volume is in drops of smaller diameter (μ m)

- $D_{0.5}$ = drop diameter such that 50% of total liquid volume is in drops of smaller diameter ($\mu\text{ m}$)
 $D_{0.9}$ = drop diameter such that 90% of total liquid volume is in drops of smaller diameter ($\mu\text{ m}$)
 r_0 = radius of laser waist (mm)

Greek symbols

- θ = crossing angle of two parallel beams (degree)
 λ = light wavelength ($\mu\text{ m}$)
 ϕ = scattering angle (degree)
 ψ = elevation angle (degree)
 Φ = Doppler difference parameter (degree)
 φ = off-axis angle (degree)
 σ = liquid surface tension (kg/s^2)

Subscripts

- D = Doppler
 e = laser source
 f = fringe
 p = particle
 r = scattering light
 x = x-direction
 y = y-direction
 z = z-direction

CHAPTER 1

INTRODUCTION

1.1 Purpose and Description

The current energy crisis which led to a skyrocketing increase in fuel prices and a global air-pollution mainly caused by the use of fossil fuels for transportation arouse many scientists and researchers to pay more attention to find alternative fuel sources. Among them, biodiesels extracted from palm, jatropa, and rapeseed become of interest due to their abundance and renewability [1]. Biodiesel can be used in diesel engines with few or no modifications. Besides having superior lubricity, biodiesel has a higher cetane number with less aromatic but higher oxygen percent by weight when compared with conventional diesel [2]. Thus, biodiesel should give less polluted emission.

To better understand the combustion of biodiesel it is necessary to conduct detailed measurements of its atomization. The required data must include the drop size and velocity distributions along the plane of injection [3]. These data could be used to design a combustion chamber in an engine or furnace. So far, to improve the combustion performance and particulate emissions, many researchers have investigated characteristics of liquid fuel spray behavior by experimental and theoretical approaches. However, there is a lack of studies about the detailed information of atomization characteristics. Therefore, different measuring techniques to obtain this information have been studied. Various techniques such as imaging techniques or hybrid light scatter detection systems combined with the Laser Doppler Velocimeter (LDV) could be employed for this task. However, the imaging method is very time consuming and it cannot provide the gas velocity information. A conventional LDV cannot discriminate signals from drops and seed particles, therefore, the gas phase measurements in polydispersions are unreliable. Light scattering methods based on the detection of scattered light intensity combined with

the LDV have not proven to be very satisfactory, particularly for applications for relatively dense sprays.

Laser-based techniques for measuring the particle-size are important in a variety of industries and to researchers in many different fields. Examples include combustion of pulverized coal and liquid fuels, spray characterization, analysis and control of particulate emissions, industrial process control and manufacture of metallic. Recently, a phase Doppler anemometer (PDA) has been successfully developed at the Center of Excellence in Particle Technology (CEPT), Chulalongkorn University and its accuracy has been verified. Thus, the laser-based technique was chosen as a tool for measuring the drop size and the velocity distribution. This thesis has benefited from a collaboration with Complex de Recherche Interprofessionnel en Aerothermochimie (CORIA), France, with more than 20 years of excellence research in optical technique. The aim of this research was to transfer research information and technology for understanding the laser-based techniques to apply in biodiesel droplet characterization.

1.2 Objective

The objective of this thesis was to study characteristics of droplets of mixture of palm oil and diesel generated by atomization with a two-fluid nozzle using a PDA to gain basic insight into its dependence on mixture composition.

1.3 Scope of Study

1.3.1 To investigate average velocity and size distribution of droplets of mixture of palm oil and diesel generated by a two-fluid nozzle using PDA technique.

1.3.2 To study the effects of density, viscosity and surface tension of blended palm oil (PO) and diesel (D) at seven different compositions, PO0:D100 (pure diesel), PO5:D95, PO10:D90, PO15:D85, PO20:D80, PO50:D50 and PO100:D0 (pure palm oil), on the droplet size and velocity.

1.3.3 To study the effects of air-pressure supplied for atomization at 0.5, 1, 1.5, 2, 3, and 4 bars on the droplet size and velocity.

1.3.4 To study the distribution of droplet size and velocity at 5 and 7 cm away from atomizer tip.

1.4 Obtained Benefits

The benefits of this research were (i) a detailed understanding of the characteristics of the spray of the mixture of palm oil and diesel created by a two-fluid nozzle, and (ii) better understanding on the application of the laser-based technique, Phase Doppler Anemometer, for droplet size and velocity measurement of liquid fuel spray. These could help to solve a part of the energy problems related to the utilization of biodiesel for our country.

The organization of the thesis is as follows:

Chapter 1 is a general introduction. The general aim of this work was presented as mentioned above of the thesis.

Chapter 2 provides a survey of applications for mixtures of vegetable oil and diesel, two-fluid atomizers. The Phase Doppler Anemometer as a technique for measuring drop and velocity is also introduced.

Chapter 3 explains the experimental setting of this research.

Chapter 4 is devoted to basic knowledge of atomization and sprays.

Chapter 5 describes the basic principles of Laser Doppler Velocimetry and the Phase Doppler Anemometer. These principles include the basics of sizing methods which are used in industry and research laboratories.

Chapter 6 discusses the experimental results which include size and velocity measurements of drops from various compositions of liquid fuels generated from a two-fluid atomizer.

Chapter 7 presents the conclusion and recommendations for further study.

CHAPTER 2

SURVEY OF APPLICATIONS

The applicability of the detailed measurements of a fuel spray for combustion needs to be studied further. The efficiency of the combustion process can be improved by understanding the mechanisms of liquid fuel atomization. More efficiency can lead to a more complete reaction and less pollution emission. The more is known on how to use energy efficiently, the more can be saved of the limited amount of energy sources. One of the new promising energy sources is vegetable oil, of which the spray information has not been investigated yet. A good understanding of the measuring techniques is needed in order to be able to investigate proper and accurate information. There are plenty of techniques to investigate fuel sprays, however all of them have different pros and cons. Consequently, the users should choose the right one to acquire the desired information.

To accomplish this goal, the spray characteristics of vegetable oil as a fuel are investigated using a Phase Doppler Anemometer. This chapter is devoted to the usability of vegetable oil as a renewable fuel, the applications of spray atomization and the applications of the phase Doppler technique in industry and in research.

2.1 Applications of Vegetable Oil as Renewable Fuel

The idea of using vegetable oils as fuel is not new. There are many advantages, for example it is renewable, energy efficient, nontoxic, and environmental friendly. Nevertheless, it has some drawbacks when used as fuel because of its common properties, such as higher viscosity and lower heat content. The most important reason to use vegetable oil as fuel is that there are many benefits for human health: smog production, which is a big problem for the elderly and young children and the emission of carbon monoxide, a poisonous gas emitted by petroleum engines, are reduced [4].

This part presents an overview on some of the literature on vegetable oil applications and their efficiency.

Altin et al. [1] presented the performance and exhaust emissions of a diesel engine using pure vegetable oils and their methyl esters. They used several types of vegetable oil, sunflower, rapeseed, cottonseed, soybean, sesame, and opium seed. The performances were shown in terms of engine torque and engine power. It was shown that vegetable oils and their esters gave less performance than commercial diesel and that more fuel was consumed. However, these renewable fuels caused less NO_x and CO_2 emission than diesel, but they gave a lot of CO emission and smoke density. They reported that the high viscosity of vegetable oil caused these results. More viscous fuel gives worse atomization in the engine. The most important advantage of vegetable oils is that they are renewable energy sources and that they are friendly for the environment.

Machacon et al. [5] studied the effect of neat coconut oil and mixtures with diesel on diesel engine performance and exhaust emissions. They found that the coconut oil had some advantages when used as combustion fuel although it has higher viscosity, density and surface tension than diesel oil, which are not good for atomization in a combustion chamber. The first advantage was that neat coconut oil did not affect the mechanical efficiency. Its operations also decreased the smoke and NO_x emissions. The ignition delay was decreased when the volume fraction of coconut oil was increased in blends. Nevertheless, these biomass-based fuels had some drawbacks on its operation. For example, the fuel consumption was higher than using diesel because it had a lower heating value. Moreover, both CO and total hydrocarbons emissions increased with increasing amounts of coconut oil in blends because of their poor characteristics.

Silvio et al. [6] studied pure palm oil used in diesel engine. Their results on engine performance showed that there was a small decrease in overall power output of the engine. Engine performance and emissions were influenced by basic differences between diesel and palm oil such as mass based heating value, viscosity, density and molecular oxygen content. The results confirmed the fact that vegetable oil gives more CO, unburned hydrocarbon and CO_2 , but less NO_x . Nevertheless, vegetable oils

are clean fuels and can be used in diesel engines without or with just small modification. It might be necessary to start the engine with pure diesel until the engine has warmed up and also heating up vegetable oil might be needed for better atomization.

Ramadhas et al. [7] found that 50-80% by volume of rubber seed oil blends with diesel gave the best performance for Compression Ignition (CI) engines without any major modification and operational difficulties. In fact, the neat rubber seed oil can be used in the engine but it causes some common problems such as poor atomization and fuel pump failure, therefore it needs to be diluted with diesel oil. It was found that blend-fueled engines had higher carbon deposits inside the combustion chamber than diesel-fueled engines because of incomplete combustion of the blended fuel.

These researches have shown that the vegetable oils are useful as renewable energy sources. They are nontoxic and environmental friendly, although their combustion efficiency is not as good as commercial diesel because of their physical properties. So, it is important to have detailed measurements of droplet sizes and droplet velocities during atomization in order to understand their combustion.

2.2 Applications of Spray Atomization

Spray atomization is widely employed within industrial and agricultural processes. Anyway, more studies about the detailed information of atomization characteristics and spray developing processes are still needed. These studies can help to improve the efficiency of combustion. They can also explain the effects of poor atomization on fouling of combustion chamber or furnace. Therefore, in view of the greater emphasis placed today on the use of clean technology, scientists and engineers need to have a better appreciation of the capabilities and performance of the individual spray nozzles. Advanced optical techniques are widely used to provide precise details of the diameter and velocity of droplets generated by individual sprays.

The following section presented some of an overview of the literature survey about spray applications and their measurement by advanced optic techniques.

Ramesh et al. [8] studied the characteristics of the atomization of a twin-fluid acoustic atomizer and combustion performance. The atomization consisted of a twin-fluid air-assist atomizer and a cavity air-jet acoustic generator. It had been used to atomize water, kerosene, diesel oil, and furnace oil. The atomizer performance was characterized in terms of the Sauter Mean Diameter (SMD), which was measured in each case using the forward diffractive light scattering technique. They found that the fluid property, viscosity, had an influence on the SMD. The SMD rose with the viscosity of the liquid. Furthermore, the atomizing air pressure had an influence on drop size distribution. When the atomizing air pressure was increased, the SMD decreased up to 300kPa; beyond that the reduction was much less significant. These characteristics were unique for this particular design of the atomizer. Studies on combustion purposes revealed the lean blow-off limits for the atomizer with kerosene as fuel.

Bachalo et al. [3] investigated the behavior of sprays generated by pressure atomizers using a Phase Doppler Particle Analyzer (PDPA). The advantage of the technique used in their work is that, unlike the scattering intensity measurement techniques, the results are unaffected by beam attenuations or slight misalignment due to beam deflections. The obtained results showed that the influence of airflow from pressure atomizer on the drop velocities and the drop traveling was significant. The injection pressure affected the measurements on both axial and radial distances.

Sindayihebura et al. [9] used a low-frequency ultrasonic atomizer to study the influence of the liquid flow rate on the spray characteristics by using a Phase Doppler Particle Analyzer (PDPA). It has many advantages, one may quote, the independent control of the spray density. In addition, it provides very fine atomization at very low liquid flow rate and has a low energy consumption. They reported the regular variation of drop size and velocity distributions with increasing liquid flow rate, symmetrical along radial distance. The distance from the nozzle has no significant effect on the stability of the drops.

Ejim et al. [10] studied the effect of surface tension and viscosity on the mean drop size profile of a spray generated by a two-phase industrial nozzle. The variation of surface tension of water was provided by adding surfactants. They reported that

there was no significant variation in the mean diameter relative to the surface tension along the spray axis at far-field spray region but at spray periphery. At this position with increasing axial distance, the mean diameter increased with decreasing surface tension. However, the mean diameter increased significantly with liquid viscosity. They also noted that studying the radial profile should not be neglected.

2.3 Applications of PDA Technique

The phase Doppler technique is a useful technique to measure the size and the velocity of droplets. The official name of this equipment depends on the company that made it. It is best known by two names, the Phase Doppler Particle Analyzer (PDPA) and the Phase Doppler Anemometer (PDA). Turning our attention on its pros and cons, the principal advantages are its high spatial resolution and the fact that the light beams do not disturb the flow. Only light needs to be transmitted to the point of interest and light from a laser can be focused into a very small volume where the velocity measurements are then performed. Furthermore, the temperature does not affect the measurement but high temperature can change the refractive index of particles, which affects the measurement accuracy. Of course there are some disadvantages of the technique as shown in Table 2.1 [11].

Table 2.1 A list of the advantages and disadvantages of the phase Doppler technique [11]

Advantages	Disadvantages
<ul style="list-style-type: none"> - Does not disturb flow - High spatial resolution - Fast response - Linear response and easily calibrated - Directional discrimination possible - Operation not usually seriously affected by temperature 	<ul style="list-style-type: none"> - Medium must be transparent - Needs scattering particles: artificial seeding may be necessary - Optical access is required: windows may have to be installed - Expensive signal processing equipment may be required in difficult situations where the signal to noise ratio is poor - Not well suited for measurements of total flow as this requires a tedious integration over a cross section

The related literature about the technique is discussed in the followings.

Boonnathee [11] developed the homemade Phase Doppler Anemometer (PDA) to measure drop sizes and velocities simultaneously at the Center of Excellence in Particle Technology, Chulalongkorn University. The laser source used in this technique was the Helium Neon laser red light with wavelength of 632.8 nm. The collecting part used two detectors to receive the light scattering signals. This equipment could measure the drop sizes in the range of 5-100 micron depending on the circular concentric diffraction array and the accuracy reached up to 65-70 percent compared to the commercial tool. Moreover, it costs only 1/10 of the commercial one.

Bachalo [12] studied the dual-beam light-scatter interferometry method to measure simultaneously the size and velocity of spherical drops. Droplets passed through the position where two laser beams were crossed and the scattered light was collected at some off-axis angle. The beam of scattered light was analyzed by the

geometric optics theory to relate the scattered fringe pattern to the droplet diameter. The use of off-axis light collection was a main key contribution in extending the particle sizing over a large size range. Their experimental results had confirmed that the technique could be applied to measure accurately the droplet size over the size range of 5 μm to 2.5 mm.

Yule et al. [13] investigated the size and velocity of droplets using back scattered light collection. They developed and modified the laser Doppler anemometer (LDA) for measuring both of size and velocity of particles. According to Mie theory, the size of particles can be determined from the relationship between amplitude of signals and diameter of drops. Air-blast was used to atomize kerosene and the drop sizes and velocities at several downstream distances were measured. At the outer region and the long distance of spray larger drops were found because of the vaporizing of liquid.



CHAPTER 3

EXPERIMENTAL

3.1 Experimental Apparatus

➤ Fuel Injection System

Figure 3.1 shows a schematic diagram of a measurement system for liquid droplet size distribution which is supplied under various injection pressures by a pneumatic pump. Liquid fuel flows under the gravity force from a medical syringe and is induced by turbulent air flow in the inlet port of the atomizer. The air is injected into the air inlet port to induce the liquid stream to form a jet. The fuel is injected at room temperature. An image of the spray system is also shown in Figure 3.2.

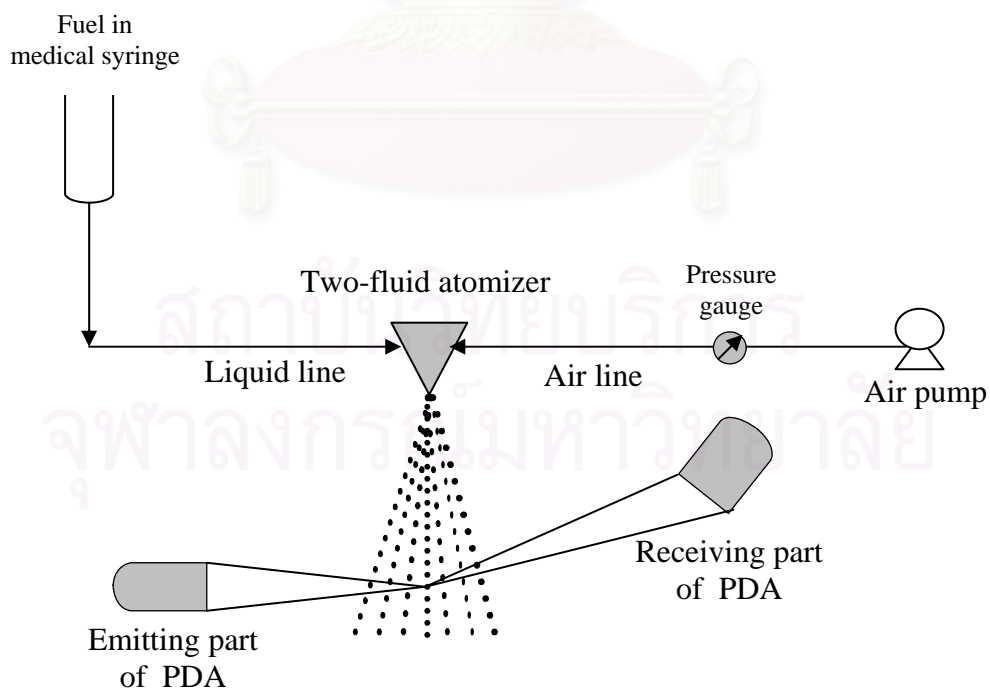


Figure 3.1 Schematic diagram of spray system

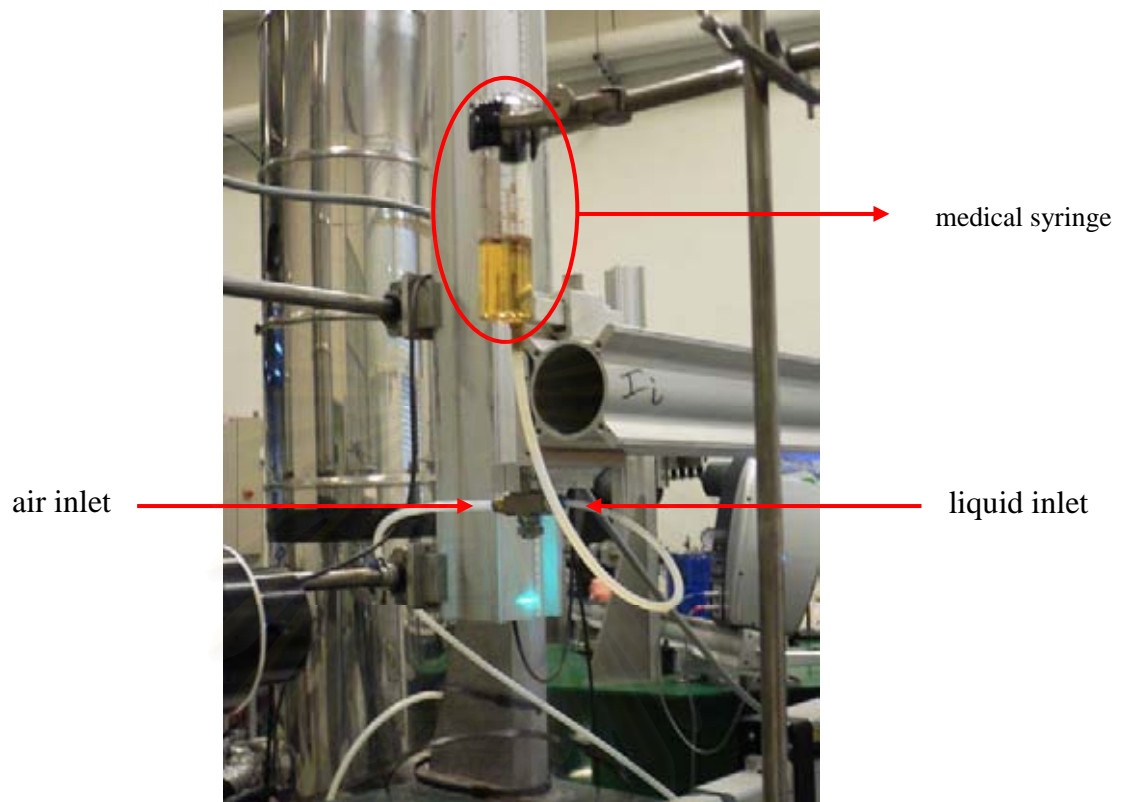
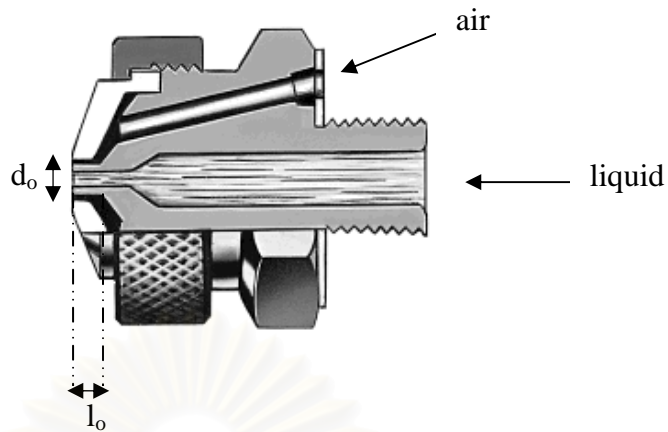


Figure 3.2 Picture of fuel injection system

➤ **Two-Fluid Atomizer**

The Two-Fluid atomizer used in this work is the external mix round spray set-ups from Pawin Engineering Co., Ltd. as shown in Figure 3.3. Figure 3.4 shows a spray set-ups with an air-cap and a fluid cap. This work used spray set-ups number 2050 and 70 for the air-cap and the fluid cap, respectively. The orifice diameter (d_o) and length (l_o) of the atomizer are 0.626 and 1.76 mm, respectively.



*Figure 3.3 Schematic diagram of external mix with siphon set-ups:
Round Spray Pattern*

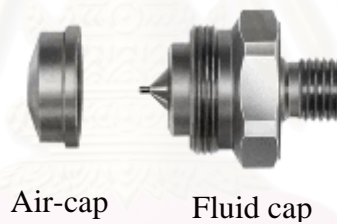


*Figure 3.4 Schematic diagram of Spray Set-ups: Each spray set-up consists of
an air-cap and fluid cap*

➤ XYZ Translation System and Stand

The three dimensional XYZ translation system (Charlyrobot Co., Ltd.) is a 3D mover. It is used to position the injector for the different measurement points for drop size measurement. Figure 3.5 shows an image of the equipment.

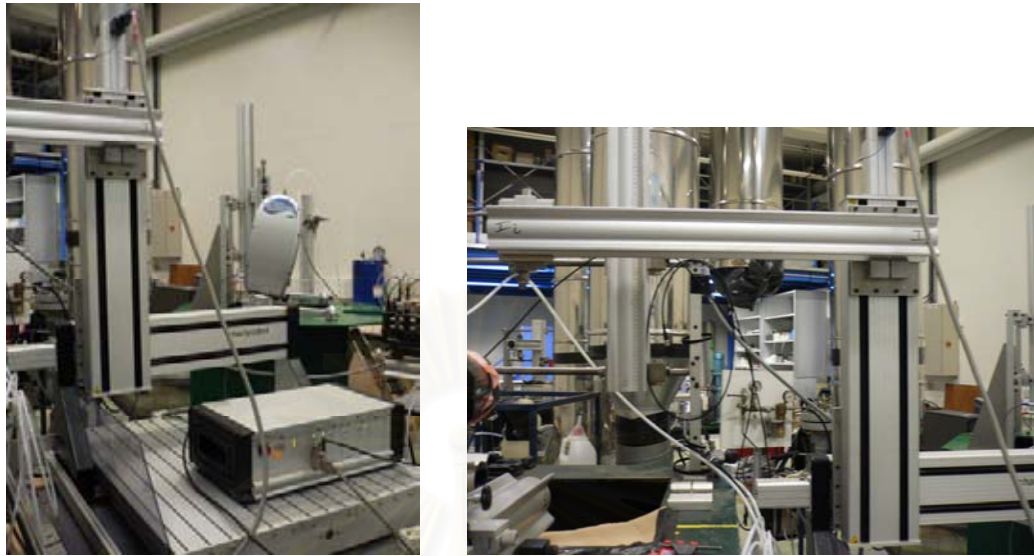


Figure 3.5 XYZ translation system and stand

➤ **Phase Doppler Anemometer (PDA)**

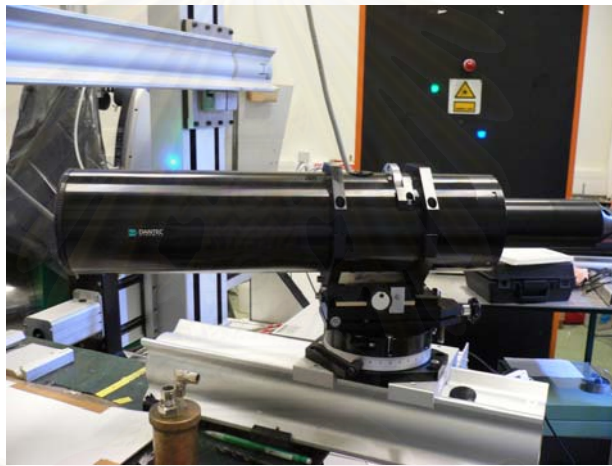
A commercial PDA system equipped with an argon ion laser (2000 mW at wavelength 488 nm, Dantec Ltd., Figure 3.6) was employed to measure the velocity and the drop size of droplets generated by a two-fluid atomizer. The PDA technique requires no calibration because the particle size and velocity are only dependent on the laser wavelength and the optical configuration.



(a)



(b)



(c)



(d)

Figure 3.6 (a) The commercial PDA (Dantec Ltd.)

(b) transmitting part

(c) collecting part

(d) laser source

The Dantec PDA configurations and parameters are presented in Table 3.1.

Table 3.1 The Dantec PDA configurations and parameters

Emitter	Receiver
Beam System U1 Wavelength : 514.5 nm Focal length : 250 mm Beam diameter : 2.2 mm Beam spacing : 40 mm	Fiber mode Scattering angle : 61 degree Receiver focal length : 310 mm Scattering mode : Refraction Aperture Mask : Mask A
Beam System U2 Wavelength : 488 nm Focal length : 250 mm Beam diameter : 2.2 mm Beam spacing : 40 mm	

➤ **Homemade PDA**

Figure 3.7 shows the schematic of the homemade PDA consisting of two parts: a transmitter and a receiver. The laser source is a Helium-Neon red light laser. The specification of the home-made PDA system used in this work is shown in Table 3.2. However, the parameters for signal processing, for example, the number of measurements and the number of points, need to be adjusted during the actual experiment to find the signal for best accuracy. The method to align the homemade PDA can be found in the master's thesis of Boonnathee [11].

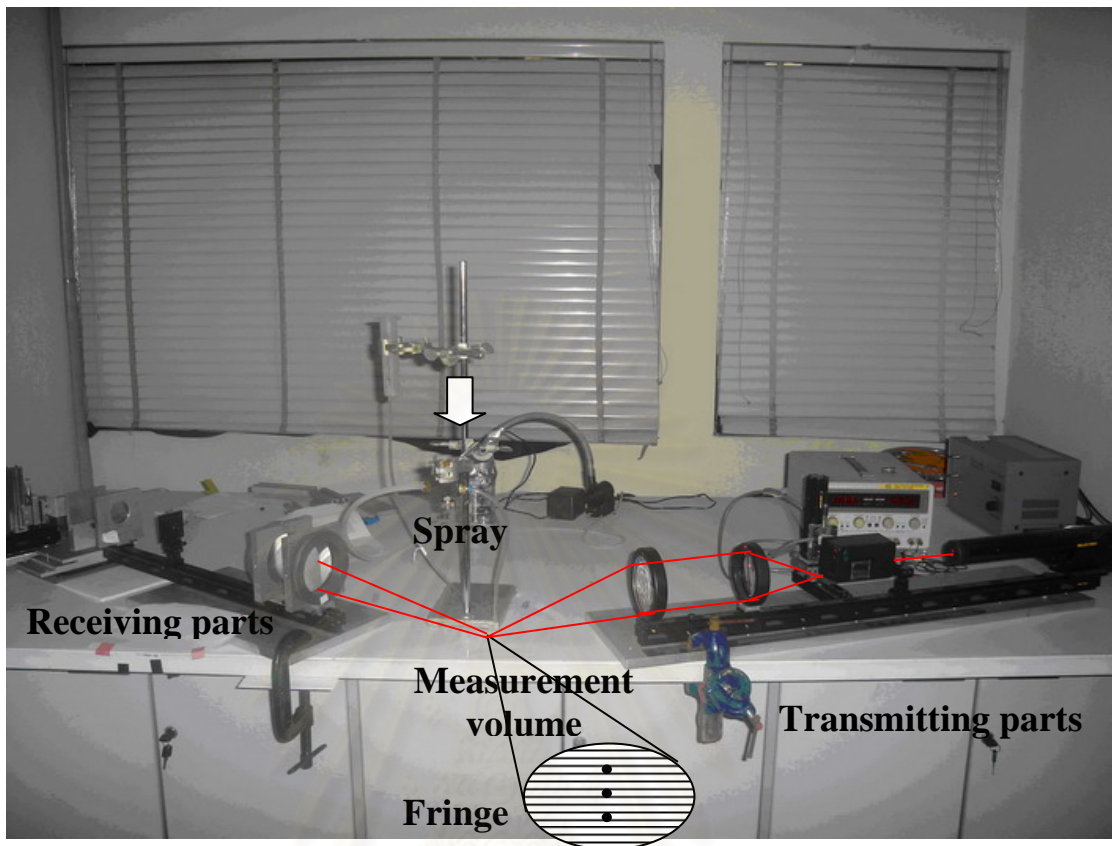


Figure 3.7 Schematic diagram of homemade PDA

Table 3.2 The specification of the homemade PDA system

Parameters	Value
Laser wavelength (nm)	632.8
Intersection angle (deg.)	4.85
Track3 (outer track)	
Fringe spacing (μm)	7.46
Track3 (outer track)	
Receiver focal length (mm)	300
Off-axis angle (deg.)	45
Elevation angle (deg.)	3.34

3.2 Fuel Preparation

Blends of vegetable oil and diesel at different compositions were used to study the effect of liquid properties. The vegetable oil that was taken into account in this work was refined palm cooking oil from a local supermarket and the diesel was commercial diesel from a local gas station. Palm cooking oil can be mixed directly with diesel fuel. The blending of vegetable oil with diesel fuel was experimented successfully by various researchers [14-16]. The blends were formulated by blending palm oil and diesel in proportions of 5:95, 10:90, 15:85, 20:80, 50:50 % (v/v). The oils were thoroughly mixed to form homogeneous blends.

In this work we define the blends to be POX:DX where PO is the palm cooking oil, D is diesel and X represents percent by volume of each liquid fuel. Table 3.3 shows the physical properties of the different liquids studied at 25 °C. Kinematic viscosities of fuels were measured by a Brookfield viscometer. Abbe refractometer model 2WAJ was used to measure refractive index. Surface tension was measured by tensiometer TVT 2LAUDA, type TVT 2-M, number 203002.

Table 3.3 The fuels properties

Fuels	Density (kg/m ³)	Kinematic Viscosity (mm ² /s)	Surface tension (kg/s ²)	Refractive index
Diesel	832.20	3.23±0.00	28.00±0.00	1.466
PO5:D95	838.38	3.49±0.01	28.02±0.05	1.467
PO10:D90	842.37	4.14±0.07	28.50±0.00	1.467
PO15:D85	846.98	4.57±0.01	28.05±0.10	1.467
PO20:D80	850.18	5.26±0.00	28.78±0.15	1.467
PO50:D50	873.23	18.06±0.01	29.90±0.20	1.468
Palm oil	895.76	57.72±0.09	33.23±0.15	1.469

3.3 Spray Characterization

The spray characteristics of the mixture of palm oil and commercial diesel were investigated by using a Phase Doppler Anemometer, which can measure local drop size and velocity simultaneously. Discharge coefficients of the atomizer with different fuels were also determined.

➤ Discharge Coefficients

The discharge coefficient of the two-fluid atomizer with different liquids is determined as follows. The mass flow rates at different injection pressures are determined by measuring liquid mass in counting time. Injection pressure is varied from 0.5 to 4 bars. The discharge coefficient (C_d) can then be calculated by

$$C_d = \frac{\dot{m}_L}{A_o \sqrt{2\rho_L P_{inj}}} \quad (3.1)$$

where \dot{m}_L and ρ_L are the mass flow rate (kg/s) and the density of the injected liquid (kg/m³), A_o is the orifice area (m²) and P_{inj} is the injection pressure (N/m²)

The maximum of the discharge coefficient can be measured with the relation of l_o/d_o . For the range of l_o/d_o between 2 to 10, Lichtarowicz et al. [16] proposed the following expression:

$$C_{D_{max}} = 0.827 - 0.0085 \frac{l_o}{d_o} \quad (3.2)$$

➤ Local drop size distribution

Local drop size distributions were measured at different axial downstream distance: 5 and 7 cm. away from the nozzle tip. The radial distribution was also studied starting from the center to the outermost position with steps of 2 mm in size. A schematic representation of the measurements is shown in Figure 3.8.

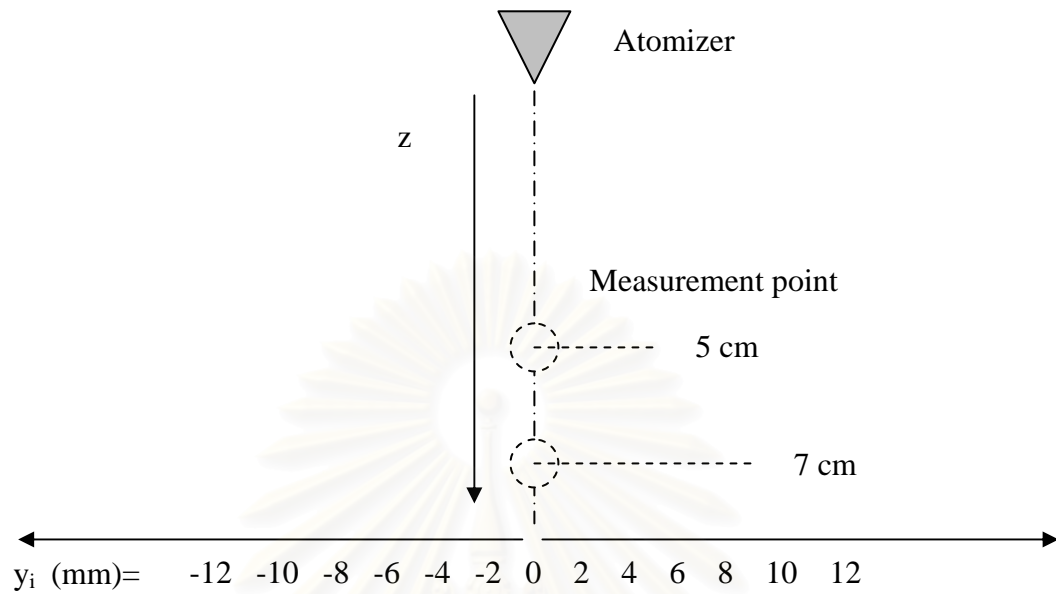


Figure 3.8 Schematic diagram of local drop size measurement

สถาบันวิทยบริการ
จุฬาลงกรณ์มหาวิทยาลัย

CHAPTER 4

ATOMIZATION AND SPRAYS

The main goal of the atomization process is to break up liquid into droplets, leading to an increase in the total surface area of the liquid. This is certainly the case for many processes, particularly those where rapid vaporization of the liquid is required. For instance, in the combustion of liquid fuels the utilization of sprays is the only choice available. The atomization quality is important for the prevention of soot and smoke formation in exhausted gases. Small droplets in the spray must travel with enough time to evaporate completely ahead of the flame front. On the contrary, larger droplets do not have such time, which results in an increased quantity of incompletely burned products. However, in other applications the increase in surface area from the atomization process may be either one of several benefits or an incidental and irrelevant result of the main process. For example, in spray painting the formation of an even surface coating takes advantage of the dispersion of droplets into a nearly homogeneous spatial pattern. Table 4.1 shows some of the most important spray applications. As the cost, complexity, atomizing performance and energy consumption vary very widely between different types of atomizers, it is important to select the proper one for any given application.

Table 4.1 Spray applications [17]

	Applications
Production or Processing	<ul style="list-style-type: none">- Spray drying (dairy products, coffee and tea, starch pharmaceuticals, soaps and detergents, pigments)- Spray cooling- Spray reactions (absorption, roasting)- Atomized suspension technique (effluents, waste liquors)- Powdered metals

	Applications
Treatment	<ul style="list-style-type: none"> - Evaporation and aeration - Cooling (spray ponds, towers, reactors) - Humidification and misting - Air and gas washing and scrubbing - Industrial washing and cleaning
Coating	<ul style="list-style-type: none"> - Surface treatment - Spray painting (pneumatic, airless, and electrostatic) - Flame spraying - Insulation, fibers, and undercoating materials - Multicomponent resins (urethanes, epoxies, polyester) - Particle coating and encapsulation
Combustion	<ul style="list-style-type: none"> - Oil burners (furnace and heaters, industrial and marine boilers) - Diesel fuel injection - Gas turbines (aircraft, marine, automotive) - Rocket fuel injection
Miscellaneous	<ul style="list-style-type: none"> - Medical sprays - Dispersion of chemical agents - Agricultural spraying (insecticides, herbicides, fertilizer solution) - Foam and fog suppression - Printing - Acid etching

Sprays can be produced in various ways. Essentially, an important issue is a high relative velocity between the liquid fuel to be atomized and the surrounding air or gas. Some atomizers accomplish these criteria by discharging the liquid at high velocity into a relatively slow-moving stream of air or gas. Notable examples include

several forms of pressure atomizers and also rotary atomizers, which eject the liquid at high velocity from the periphery of rotating cup or disk. An alternative approach is to expose the relatively slow-moving liquid to a high-velocity air stream. The latter method is generally known as twin-fluid, air-assist, or airblast atomization [17].

Some basic knowledge of atomization and sprays will be reported in this chapter. It consists of the basic process in atomization, drop size distribution and spray, and various types of atomizers.

4.1 Basic process in atomization

Studying the mechanisms of the atomization process is difficult because the process is very fast. Most of the time researchers use image techniques to capture the microscopic images for investigation of the mechanisms. The exact mechanism depends upon the particular form of atomizer being considered and the nature of the liquid being atomized, but the basic mechanism always involves the formation of unstable columns of liquid which break down into rows of droplets.

Breakup of drops

When atomization occurs as a result of interaction between a liquid and the surrounding air, the overall atomization process involves several interacting mechanisms, including the splitting of the larger drops during the final stages of disintegration. Therefore it is of interest to examine the various ways in which a single drop of liquid can break up under the action of aerodynamic forces.

A rigorous mathematical solution for the breakup of a drop would demand an exact knowledge of the distribution of aerodynamic pressures on the drop. However, as soon as the drop is deformed by these pressures, the pressure distribution around it also changes and either a state of equilibrium between the external aerodynamic forces and the internal forces due to surface tension and viscosity is attained or further deformation follows, leading to possible breakup of the drop.

Under equilibrium conditions the internal pressure at any point on the drop surface, p_l , is sufficient to balance the external aerodynamic pressure, p_A , and the surface tension pressure p_σ so that

$$p_l = p_A + p_\sigma = \text{constant}$$

Note that for a spherical drop

$$p_\sigma = \frac{4\sigma}{D}$$

A drop can remain stable as long as a change in air pressure at any point on its surface can be compensated by a corresponding change in p_σ such that p_l remain constant. However, if p_A is large compared with p_σ then any appreciable change in p_A cannot be compensated by a corresponding change in p_σ to maintain p_l constant. In this situation, the external pressure p_A may deform the drop to an extent that leads to further reduction in p_σ and finally to disruption of the drop into smaller drops.

These considerations lead to the concept of a critical drop size. For drops slightly larger than the critical size, the breakup time increases for decreasing size, until the stable drop has an infinite breakup time. The influence of liquid viscosity, by opposing deformation of the drop, is to increase the breakup time. If the aerodynamic force on the drop declines during the breakup time, no breakup may occur, although the initial aerodynamic force was large enough to produce breakup.

In case of twin-fluid atomizers which are used in this work, Williams [18] has described the basic processes of their atomization to be the three stages shown in the following section.

Twin-Fluid Atomizers

In twin-fluid atomizers a high velocity gas stream impinges on a relatively slowly moving liquid fuel stream, and the process of atomization can be considered to consist of the following stages:

(i) Formation of thin liquid sheets along the inner walls of an internal-mixed atomizer, or of free sheets of liquid, or of fine jets.

(ii) Disintegration of these sheets or jets by aerodynamic forces to form ligaments and/or large droplets.

(iii) Breakup of the ligaments and large droplets to form a spray.

Whether jets or sheets are produced their breakup in a twin-fluid atomizer is much more controlled by the air flow than is the case in a pressure jet atomizer.

4.2 Drop Size Distribution and Sprays

Most practical atomizers generate drops in the size range from a few micrometers up to around 500 μm . Some kind of atomizers can produce uniform drops. Nevertheless, some of them generate varying size of particles. Therefore, it is necessary to represent the created drops in a proper way to recognize the characteristics of the spray.

4.2.1 Graphical Representation of Drop Size Distribution

An instructive picture of the drop size distribution may be obtained by plotting a histogram of the drop size, each ordinate representing the number of drops. A typical histogram of this type is shown in Figure 4.1. If instead of plotting the number of drops, the volume of the spray is plotted as a histogram of drop size, the resulting histogram is skewed to the right, as shown in Figure 4.2.

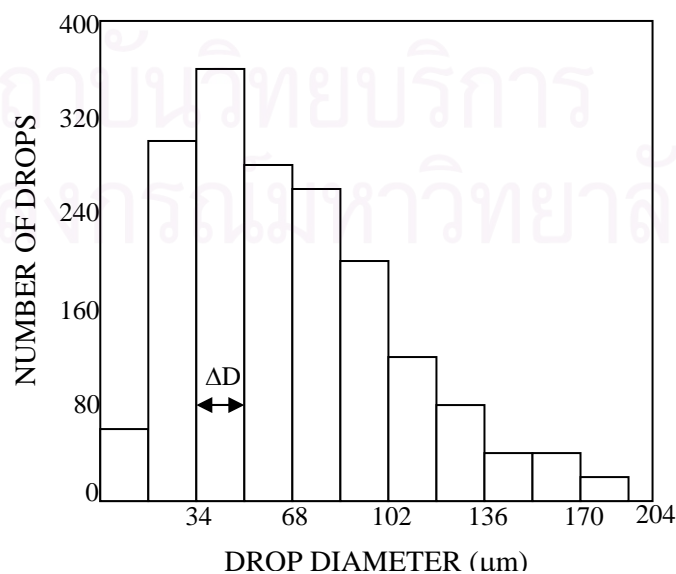


Figure 4.1 Typical drop size histogram

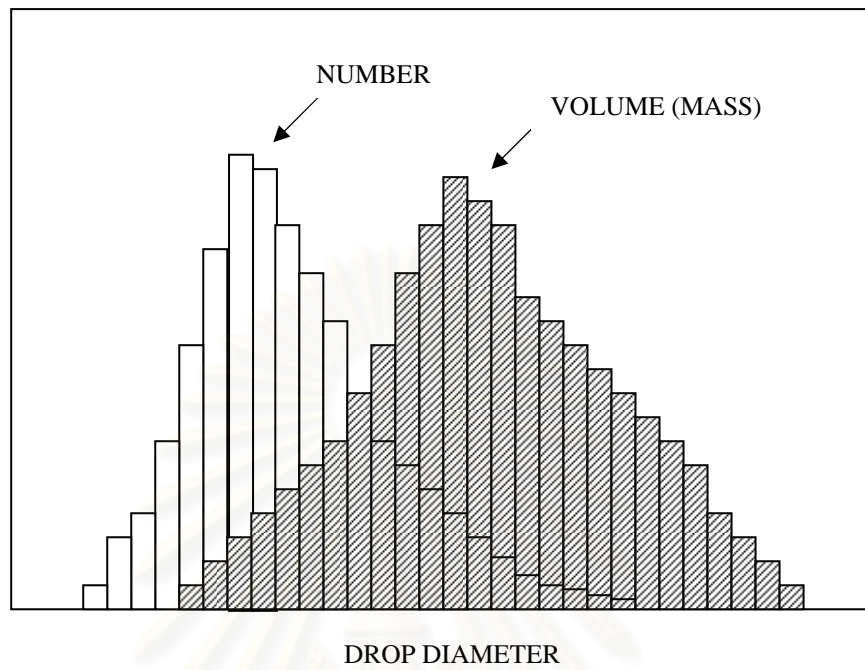


Figure 4.2 Drop size histogram

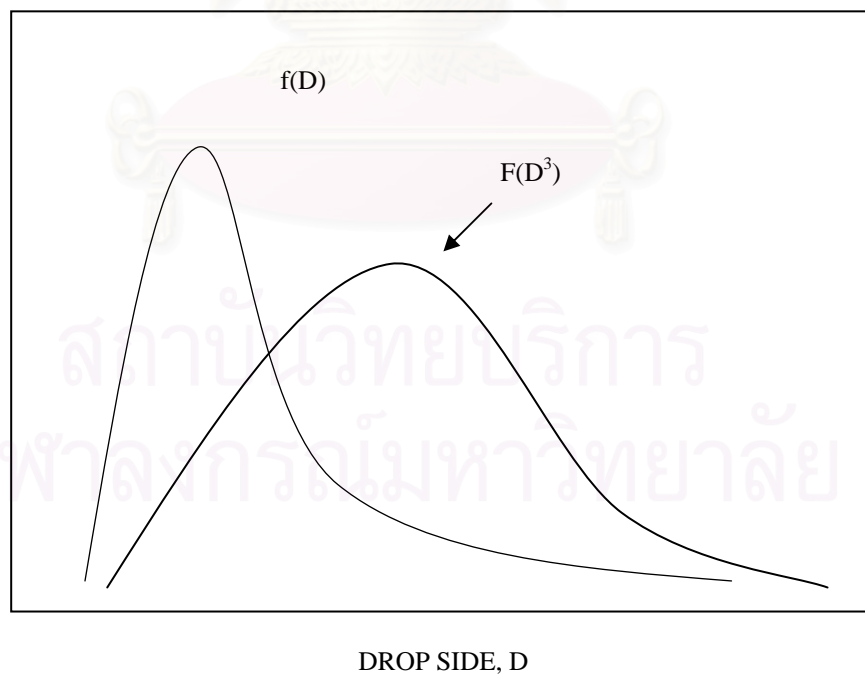


Figure 4.3 Drop size frequency distribution curve

As ΔD is made smaller, the histogram assumes the form of a frequency curve that may be regarded as a characteristic of the spray, provided it is based on sufficiently large samples. Such a curve, shown in Figure 4.3, is usually referred to as a frequency distribution curve. The ordinate values may be expressed in several alternative ways: as the number of drops with a given diameter, the relative number or fraction of the total, or the fraction of the total number per size class. If the ordinate is expressed in the last manner, the area under the frequency distribution curve must be equal to 1.0.

If the surface area or volume of the drops in the spray is plotted versus the diameter, the distribution curve is again skewed to the right, as shown in Figure 4.3, due to the weighting effect of the larger diameter.

In addition to representing the drop size distribution with a frequency plot, it is also informative to use a cumulative distribution representation. This is essentially a plot of the integral of the frequency curve, and it may represent the percentage of the total number of drops in the spray below a given size or the percentage of the total surface area or volume of a spray contained in drops below a given size. Cumulative distribution curves plotted on arithmetic coordinates have the general shape shown in Figure 4.4; the ordinate may be the percentage of drops by number, surface area, or volume.

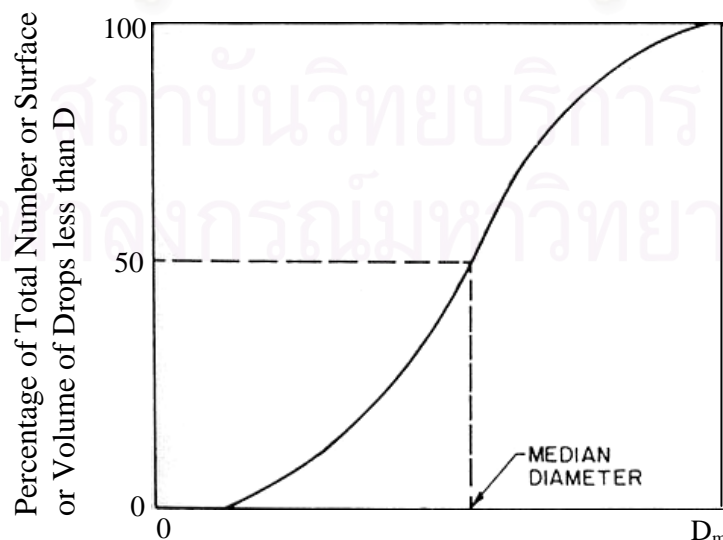


Figure 4.4 Cumulative drop size distribution curve [17]

4.2.2 Mean Diameters

In many calculations of mass transfer and flow processes it is convenient to work only with the mean or average diameter instead of the complete drop size distribution. One of the most common mean diameters is D_{10} , where

$$D_{10} = \frac{\int_{D_0}^{D_m} D(dN/dD)dD}{\int_{D_0}^{D_m} (dN/dD)dD} \quad (4.1)$$

Other mean diameters of interest include the

$$\text{Surface mean: } D_{20} = \left[\frac{\int_{D_0}^{D_m} D^2 (dN/dD)dD}{\int_{D_0}^{D_m} (dN/dD)dD} \right]^{1/2} \quad (4.2)$$

$$\text{Volume mean: } D_{30} = \left[\frac{\int_{D_0}^{D_m} D^3 (dN/dD)dD}{\int_{D_0}^{D_m} (dN/dD)dD} \right]^{1/3} \quad (4.3)$$

In general, we have

$$(D_{ab})^{a-b} = \frac{\int_{D_0}^{D_m} D^a (dN/dD)dD}{\int_{D_0}^{D_m} D^b (dN/dD)dD} \quad (4.4)$$

where a and b may take on any values corresponding to the effect under investigation, and the sum a + b is called the order of the mean diameter.

Equation (4.4) may also be written as

$$D_{ab} = \left[\frac{\sum N_i D_i^a}{\sum N_i D_i^b} \right]^{1/(a-b)} \quad (4.5)$$

where i donates the size range considered, N_i is the number of drops in size range i , and D_i is the middle diameter of size range i . Thus, for example, D_{10} is the linear average value of all the drops in the spray; and D_{32} (SMD) is the diameter of the drop whose ratio of volume to surface area is the same as that of the entire spray. These and other important mean diameters are listed in Table 4.2.

Table 4.2 Mean Diameters and their Applications [17]

a	b	(a+b) order	Name of Mean Diameter	Expression	Application
1	0	1	Length	$\frac{\sum N_i D_i}{\sum N_i}$	Comparisons
2	0	2	Surface Area	$\left(\frac{\sum N_i D_i^2}{\sum N_i} \right)^{1/2}$	Surface area controlling
3	0	3	Volume	$\left(\frac{\sum N_i D_i^3}{\sum N_i} \right)^{1/3}$	Volume controlling, e.g. hydrology
2	1	3	Surface area-length	$\frac{\sum N_i D_i^2}{\sum N_i D_i}$	Absorption
3	1	4	Volume-length	$\left(\frac{\sum N_i D_i^3}{\sum N_i D_i} \right)^{1/2}$	Evaporation, molecular diffusion
3	2	5	Sauter (SMD)	$\frac{\sum N_i D_i^3}{\sum N_i D_i^2}$	Mass transfer, reaction
4	3	7	De Brouckere or Herdan	$\frac{\sum N_i D_i^4}{\sum N_i D_i^3}$	Combustion equilibrium

4.2.3 Representative Diameters

For most engineering purposes the distribution of drop sizes in a spray may be represented concisely as a function of two parameters, one of which is a representative diameter and the other a measure of the range of drop sizes.

There are many possible choices of representative diameter, each of which could play a role in defining the distribution function. The various possibilities include the following:

$D_{0.1}$ = drop diameter such that 10% of total liquid volume is in drops of smaller diameter

$D_{0.5}$ = drop diameter such that 50% of total liquid volume is in drops of smaller diameter

$D_{0.9}$ = drop diameter such that 90% of total liquid volume is in drops of smaller diameter

The relative span factor, which can be used to indicate the spread of drop sizes in a spray, can be calculated from these representative diameters by

$$span = \frac{D_{0.9} - D_{0.1}}{D_{0.5}} \quad (4.6)$$

4.3 Atomizers

In this section the general features of the main types of atomizers for industrial and laboratory use are described. Primary emphasis is placed on the atomizers used in combustion equipment. Most of the fuels employed in heat engines and industrial furnaces are liquids which must be atomized before injection into the combustion zone. The process of atomization produces a very high ratio of surface to mass in the liquid phase, therefore promoting rapid evaporation and high rates of combustion.

Lefebre [17] showed the characteristics of an ideal atomizer, it would have to possess:

- Ability to provide good atomization over a wide range of liquid flow rates

- Rapid response to change in liquid flow rate
- Freedom from flow instabilities
- Low power requirements
- Capability for scaling, to provide design flexibility
- Low cost, light weight, ease of maintenance, and ease of removal for servicing
- Low susceptibility to damage during manufacture and installation

And fuel atomizers should have all the above features, plus the following:

- Low susceptibility to blockage by contaminants and to carbon buildup on the atomizer face
- Low susceptibility to gum formation by heat soakage
- Uniform radial and circumferential fuel distribution

4.3.1. Pressure Atomizers

As the name indicates, pressure atomizers depend on the conversion of pressure into kinetic energy to achieve a high relative velocity between the liquid and the surrounding gas. Most of the general atomizers are of this type. Several types of pressure atomizers are described below.

➤ Plain Orifice

The sprays produced by plain-orifice atomizers have a cone angle that usually lies between 5° and 15° . This cone angle is only slightly affected by the diameter and length/diameter ratio of the orifice and is mainly dependent on the viscosity and surface tension of the liquid and the turbulence of the issuing jet. An increase in turbulence increases the ratio of the radial to the axial component of velocity in the jet and thereby increases the cone angle. Plain-orifice nozzles are widely used as a mean of introducing liquid into a flowing stream of air or gas. Two cases of practical importance are (1) injection into a coflowing or contraflowing stream of air and (2) transverse injection across a flowing stream of air.

➤ Simplex

The narrow spray cone angles exhibited by plain-orifice atomizers are disadvantageous for most practical applications. Much wider cone angles are achieved in the simplex or pressure-swirl atomizers, in which a swirling motion is imparted to the liquid so that, under the action of the centrifugal force, it spreads out in the form of a cone as soon as it leaves the orifice.

There are two basic types of simplex nozzles. One type is a solid-cone spray which is comprised of drops that are distributed fairly uniformly throughout its volume. The other nozzle type produces a hollow-cone spray, in which most of the drops are concentrated at the outer edge of a conical spray pattern. These two spray structures are illustrated in Figure 4.5.

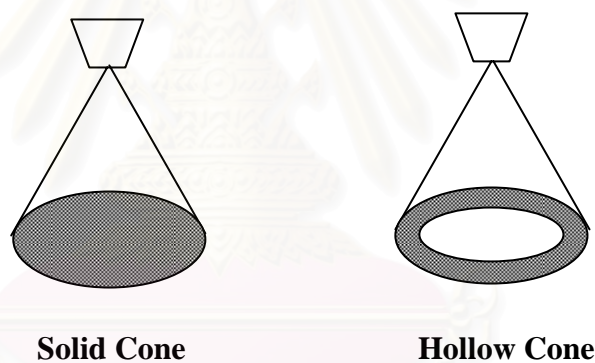


Figure 4.5 Spray structures produced by Simplex or pressure-swirl atomizer

➤ Fan Spray Nozzles

These atomizers are used in the coating industry, in some small annular gas turbine combustors, and in other applications where a narrow elliptical pattern is more appropriate than the normal circular pattern. The spray is formed by arranging for a round liquid jet to impinge on a curved surface. This arrangement produces a wide, flat, relatively coarse spray pattern containing a fairly uniform distribution of drops. The nominal spray pattern is 120° or more, depending on size of the atomizer. In general, drop sizes from fan spray atomizers are larger than those from swirl spray atomizers of the same flow rate.

4.3.2. Rotary Atomizers

In this type of atomizer, liquid is fed onto a rotating surface, where it spreads out fairly uniformly under the centrifugal force. There are various kinds of rotating surfaces, for instance, a flat disk, cup, and slotted wheel. Several mechanisms of atomization are observed with a rotating flat disk, depending on the flow rate of the liquid and the rotating speed of the disk. The liquid spreads out across the surface and it centrifuged off as discrete drops of uniform size, each drop drawing behind it a fine ligament. The larger diameters of drops are observed when the liquid flow rate is increased. The rotary atomizers are used in industrial spray-drying operation.

4.3.3 Air-Assist Atomizers

For internal-mixing atomizers, the spray cone angle is a minimum for maximum airflow, and the spray widens as the airflow is reduced. This type of atomizers is very suitable for highly viscous liquids, and good atomization can be obtained down to very low liquid flow rates. External-mixing types can be designed to give a constant spray angle at all liquid flow rates. However, their utilization of air is less efficient, and consequently their power requirements are higher. Both types of air-assist atomizers types are shown in Figure 4.6 and 4.7.

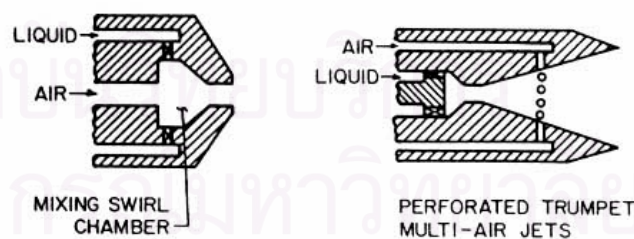


Figure 4.6 Internal-mixing air-assist atomizers [17]

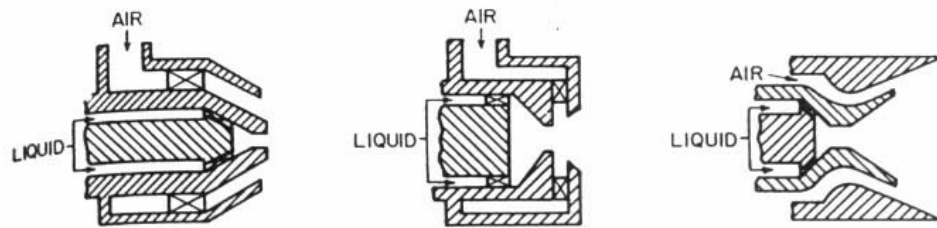


Figure 4.7 External-mixing air-assist atomizers [17]

4.3.4 Airblast Atomizers

The airblast atomizer function works in exactly the same manner as air-assist atomizer; both employ the kinetic energy of a flowing air stream to shatter the fuel jet or sheet into ligaments and then drops. The main differences between the two systems are the quantity of air employed and its atomizing velocity.

Airblast atomizers have many advantages over pressure atomizers, especially in their application to combustion systems operating at high pressure. They require lower fuel pump pressure and produce a finer spray. The advantages of the airblast atomizer have led to its installation in a wide variety of aircraft, marine, and industrial gas turbine. Most of the systems in service are of the prefilming type, in which the liquid is first spread out in a thin continuous sheet and then subjected to the atomizing action of high-velocity air. An example of prefilming type is shown in Figure 4.8.

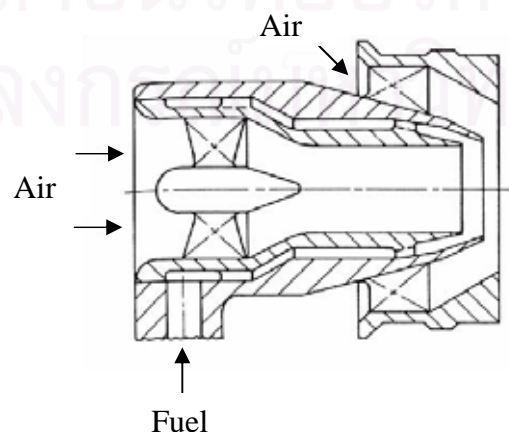


Figure 4.8 Prefilming airblast atomizer [17]

4.3.5 Electrostatic Atomizers

The basic idea of this type of atomizer is to make some area of its surface unstable. Then, the surface will break into ligaments, which disintegrate into drops. In electrostatic atomization, the energy causing the surface to disrupt comes from the mutual repulsion of like charges that have accumulated on the surface. An electrical pressure is created that tends to expand the surface area. This pressure is opposed by surface tension forces, which tend to contract or minimize surface area. When the electrical pressure exceeds the surface tension forces, the surface becomes unstable and droplets formation begins.

4.3.6 Ultrasonic Atomizers

When a liquid is introduced onto a rapidly vibrating solid surface, a checkerboard-like wave pattern appears in the film that forms as the liquid spreads over the surface. A useful attribute of the ultrasonic atomizer is its low spray velocity. This makes it an easy matter to entrain the spray in a moving stream and convey the drops in a controlled manner as a uniform mist. This is especially important in coating applications and in such processes as humidification, product moisturizing, and spray drying. The schematic of this type of atomizer is shown in Figure 4.9.

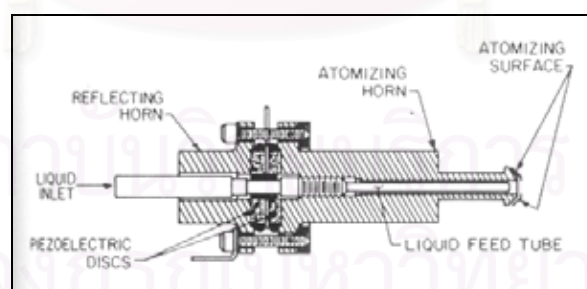


Figure 4.9 Ultrasonic nozzle assembly [17]

Lefebvre [17] also classified types of atomizers and showed advantages, disadvantages and some of applications as in Table 4.3.

Table 4.3 Summary the types of atomizers

Type	Advantages	Drawbacks
1. Pressure Atomizer 1.1 Plain orifice 1.2 Simplex 1.3 Fan spray	1. Simple, cheap 2. Rugged 1. Simple, cheap 2. Wide spray angle (up to 180°) 1. Good atomization 2. Narrow elliptical pattern sometime advantageous	1. Narrow spray angle 2. Solid spray cone 1. Needs high supply pressure 2. Cone angle varies with pressure difference and ambient gas density 1. Needs high supply pressure
2. Rotary 2.1 Spinning disk 2.2 Rotating cup	1. Nearly uniform atomization possible with small disks rotating at high speed 2. Independent control of atomization quality and flow rate 1. Capable of handling slurries	1. Produces a 360° spray pattern 1. May require air blast around periphery
3. Air-assist 3.1 Internal Mixing 3.2 External-mixing	1. Good atomization 2. Large passages prevent clogging 3. Can atomize high-viscosity liquid 1. Same as internal mixing, plus construction prevents	1. Liquid can back up in air line 2. Requires auxiliary metering device 3. Needs external source of high pressure air or steam 1. Needs external sources of air

Type	Advantages	Drawbacks
	backing up of liquid into the air line	2. Does not permit high liquid/air ratios
4. Airblast		
4.1 Plain jet	1. Good atomization 2. Simple, cheap	1. Narrow spray angle 2. Atomizing performance inferior to prefilming air blast
4.2 Prefilming	1. Good atomization especially at high ambient air pressure	1. Atomization poor at low air velocities
5. Electrostatic	1. Very fine atomization	1. Cannot handle high flow rates
6. Ultrasonic	1. Very fine atomization 2. Low spray velocity	1. Cannot handle high flow rates

CHAPTER 5

MEASUREMENT TECHNIQUES

Detailed measurements of velocities and sizes of drops in two-phase flow processes are necessary for process and quality control. Aims of such measurements are to characterize the global flow behavior and flow regimes, and to obtain local information about the characteristic properties of such flows. Moreover, experimental techniques are required to analyze behavior and motion of individual particles in order to assess microprocesses occurring on the scale of the particles.

This chapter is devoted to the optic techniques which are employed to measure size and velocity of atomized droplets. In the first part basic knowledge of measurement techniques is summarized. The emphasis will be on the droplet size and velocity distributions. The second part of this chapter consists of the theory on Laser Doppler Velocimetry (LDV) and the Phase Doppler Anemometer (PDA) which are used in this work.

5.1 Experimental Methods for Determining Droplet Size Distribution

It is important to determine droplet sizes in terms of the numbers of droplets in a particular size range. Also it should be noted that the size distribution of a spray varies with downstream distance from an atomizer tip.

The most common used sizing techniques are described in this section. Lefebvre [17] divided the drop sizing methods into mechanical, electrical and optical methods.

5.1.1 Mechanical Methods

➤ The Frozen Drop and Wax Method

These are old but still useful techniques in which the atomized spray is directly measured as solid particles. In the frozen droplet technique the spray is

injected into an alcohol or acetone bath which is maintained at the temperature of dry ice. The frozen particles so produced can then be sized either simply by sieving, or by photographing the particles and counting them later using an enlarged photograph, or by means of an automatic particle counting and sizing technique. Of the automatic techniques available one convenient method involves the use of a commercial image analyzer in which the sample may be examined directly by a microscope system or photographs.

The wax method is dependent upon the fact that paraffin wax, when heated to an appropriate temperature above its melting point, has properties such as viscosity, surface tension, etc., which are similar to many liquid fuels. In the application of this method molten paraffin wax at the appropriate temperature is pumped to the spray nozzle and the wax spray so produced is directed into water in order to solidify the droplets produced. The solid wax particles are again collected and sized by passing them through a series of graded gauge sieves.

➤ **Collection of Drops on Slide**

This is one of the most simple techniques which collects the sample of a spray on a glass microscope slide and makes a microscopic examination of some droplets. The slides need to be coated by a magnesium oxide in order to cause indentation. The sizes of the indentations may be measured automatically but they have to be corrected for the effect of flattening on impact. There are many disadvantages for measuring the droplets size. For instance, some part of the slide is not covered with droplets so multiple impactions are possible and if there are not so much drops on the slide they may not demonstrate the characteristic of the spray. Also the volatile liquid spray might evaporate before impact on the slide which means that not all drops can be measured.

➤ **Collection of Drops in Cells**

An improvement on the coated-slide technique is one in which the drops are caught on a target where they are held suspended while they are counted and measured. This method has three advantages over collecting on a slide: (1) the drops

remain almost perfectly spherical, (2) evaporation is prevented, and (3) provided no splitting of the drop occurs on hitting the immersion liquid, the true sizes of the drops are obtained and can be measured directly. However, this method can not be applied satisfactorily to coarse sprays due to the risk of disintegration of the largest drops on impact with the immersion liquid.

5.1.2 Electrical methods

Electric methods generally rely on the detection and analysis of electronic pulses produced by drops for calculating size distribution.

➤ Charge Wire Technique

This technique operates on the principle that when a drop impinges on an electrically charged wire it removes an amount of charge that depends on its size. This allows drop sizes to be obtained by converting the charge transfer into a measurable voltage pulse.

➤ Hot Wire Technique

When a liquid drop becomes attached to a heated wire it causes local cooling of the wire as it evaporates. The device employed is a constant-temperature hot wire anemometer. When no drops are presented, the electrical resistance of the wire is high and sensibly uniform along its length. When a drop attaches to the wire, local cooling by the drop reduces the resistance in proportion to the drop size. This reduction in resistance is manifested as a voltage drop across the wire supports.

5.1.3 Optical methods

Optical methods can be divided into imaging and nonimaging types. The drops can be seen as they exist at the point and time where knowledge of their size is required in the imaging methods. The most popular methods are nonimaging because they have a fast response and high accuracy.

➤ **High-Speed Photography**

It involves taking a photograph with a light pulse of sufficient intensity and sufficient short duration to produce a sharp image and then counting and sizing the images on the processed film. It can also be used to obtain information on drop velocities. If two light pulses are generated in rapid succession, a double image is obtained of a single drop on the photographic plate, from which the velocity of the drop can be determined by measuring the distance traveled by the drop and dividing it by the time interval between the two pulses.

➤ **Holography**

With this method a sample volume of moving drops is illuminated with a coherent beam of light in the form of a short pulse. The measurement volume is a cylinder with length equal to the total width of the spray at the particular axial station and with diameter equal to that of the laser beam. As the duration of the laser pulse is extremely short (20 ns), the drops contained within the measurement volume are effectively frozen. The resulting hologram provides a complete three-dimensional image of the spray in which drops as small as 15 μm are clearly visible. The hologram can then be illuminated with a coherent beam of light to produce a stationary image of all the drops at their correct relative locations in space. Thus, the holographic method is essentially a two-step imaging process that captures in permanent form the size and location of a moving system of drops and then produces a stationary three-dimensional image of all drops contained within the sample volume.

➤ **Light-Scattering Technique**

The optical properties of a medium are characterized by its refractive index, and as long as this is uniform, light will pass through the medium undeflected. When there is a variation of the refractive index because of the particles present, part of the radiation will be scattered in all directions. In drop size analysis, provided the number of drops under observation is large enough to ensure that a representative sample is obtained, the properties of the scattered light can be used to indicate the drop size distribution.

5.2 Measurement of Droplet Velocity

➤ Direct Photography

In this case the opening of the camera shutter is used to trigger one flash and then, after an appropriate interval controlled by an electronic time delay unit, the second flash unit discharges after which the camera shutter closes. The resulting photograph now consists of a series of double images, each pair corresponding to each droplet. From the separation of each pair of images and from the knowledge of the time interval the droplet velocity and direction may be deduced.

➤ Laser Doppler Anemometer (LDA) (or Laser Doppler Velocimeter (LDV))

Information on droplet velocities may also be deduced by well developed and commercially available laser-anemometer techniques in which a moving particle influences the optical properties of two crossed laser beams. The data obtained on the particle velocity relate entirely to the small volume where the two split beams intersect.

In this work we chose the Phase Doppler Anemometer to measure drop sizes and velocities because of several reasons. First, it can be used to measure very accurately and give fast responses. Second, it doesn't disturb the spray. Finally, the Center of Excellence in Particle Technology has a good collaboration with Complexe de Recherche Interprofessionnel en Aérothermochimie (CORIA), France, with more than 20 years of excellence research in optical technique, therefore we could transfer the knowledge for understanding the laser-based techniques.

In the following section we will show the basic theory of laser-based techniques which relate to the sizing method in this work. Laser Doppler Velocimetry (LDV) is used to measure velocity of drops. The Phase Doppler Anemometer is developed from LDV to be able to measure velocity and size of drops simultaneously. Thus, both techniques need to be understood.

5.3 Laser Doppler Velocimetry (LDV)

As a basic tool for analyzing dynamic characterisation of atomized droplets or diffusing particles, a Laser Doppler Anemometer is employed to measure droplets' or particles' velocity at a point in a flow using light beams. This technique is based on the determination of the velocity of fine tracer particles, which follows the fluid flow practically without delay.

The spatial resolution is given by the size of measurement volume, which is defined by the intersection of the two laser beams. The beams are produced by splitting one laser beam into two parallel beams, which are focused symmetrically by a lens. The resulting beams cross each other with the angle 2α , as shown in Figure 5.1. The focus of each beam is in the centre of the measurement volume. When a tracer particle passes the measurement volume, part of the scattered light is collected by a lens and detected by a sensor [19].

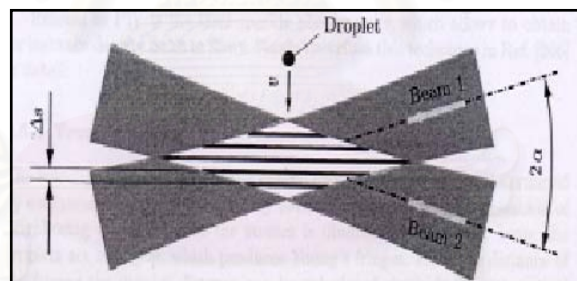


Figure 5.1 Crossing of two laser beams with angle 2α [19]

The physical principle of LDV for velocity measurement is the Doppler Effect, which relates the interaction of sound or light waves received by a stationary observer from a moving emitter. In LDV this principle is used in such a way that a laser emits plane light waves which are transmitted from a moving emitter, the particle. Hence, the frequency or wavelength of the light received by the particle is already modulated. Since the moving particle scatters the light into space, an additional Doppler shift occurs when the scattered light is received by a stationary observer. The principle of LDV can be explained using a fringe model. When the two

coherent light beams cross, the interference of the light waves result in a fringe pattern parallel to the bisector plane (i.e. the x-z plane in Figure 5.2) which can be visualized when a lens is placed at the intersection of two beams. As the particle passes through the LDV probe volume, the fringe, the scattering intensity was detected by a photodetector. The fringe spacing (d_f) is basically the conversion factor to determine the particle velocity (v) from the measured Doppler frequency (f_D).

$$v = \frac{d_f}{f_D} \quad (5.1)$$

The spatial resolution of the velocity measurement depends on the dimensions of the LDA probe volume which is determined by the initial laser beam diameter, the angle between the crossing beams, the focal length of the receiving lens and the off-axis angle. The incident focused laser beams have a Gaussian intensity distribution as shown in Figure 5.2; their waist diameter at the focal plane is taken to be that value at which the light intensity has diminished to $1/e^2$ of the maximum value at the beam axis [19]. The waist diameter (d_m) is given by

$$d_m = \frac{4 f_e \lambda_e}{\pi d_0} \quad (5.2)$$

where (λ_e) is wavelength of laser light, d_0 is the $1/e^2$ unfocused laser beam diameter and f_e is the transmitting lens focal length. The probe volume established by the two crossing beams has an ellipsoidal shape as shown in Figure 5.2. The dimensions of the $1/e^2$ ellipsoid, shown in Figure 5.2, are given by

$$\Delta x = \frac{d_m}{\cos \theta} \quad (5.3)$$

$$\Delta y = d_m \quad (5.4)$$

$$\Delta z = \frac{d_m}{\sin \theta} \quad (5.5)$$

$$N_f = \frac{8}{\pi} \frac{f_c}{d_0} \tan \theta = \frac{4}{\pi} \frac{\Delta b}{d_0} \quad (5.6)$$

where θ is the reference beam angle, N_f is the number of fringes in the measurement volume and Δb is the initial spacing of the transmitting lens.

A typical optical setup of an LDA system operated in the forward scattering mode is shown in Figure 5.3. The transmitting optics consist of the laser, a beam splitter and a transmitting lens. The receiving optics consist of an imaging lens with a mask in front of it and a photodetector with a pinhole.

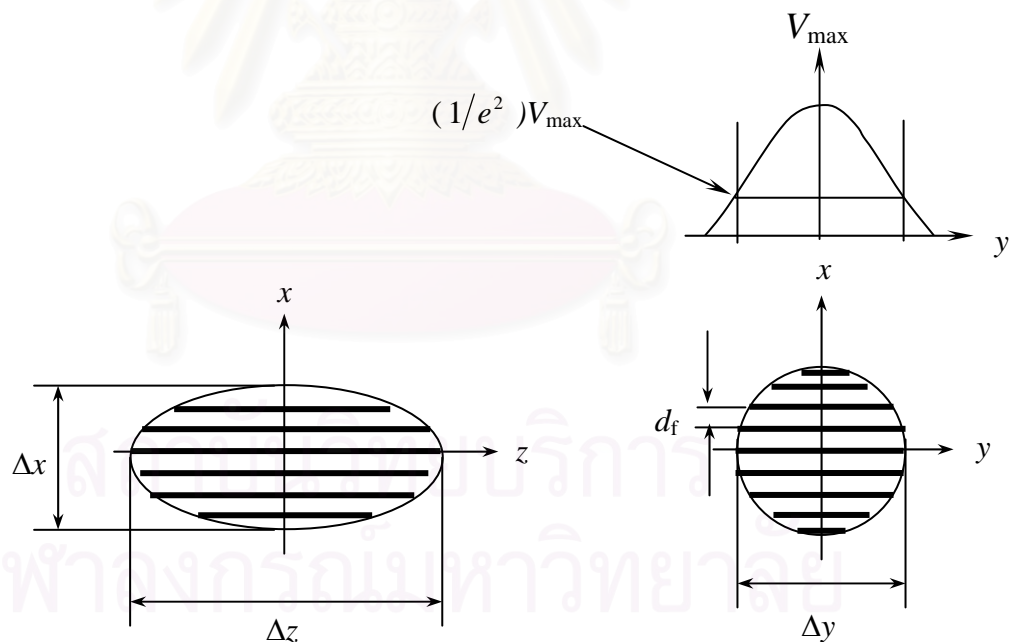


Figure 5.2 Dimensions of LDA probe volume [19]

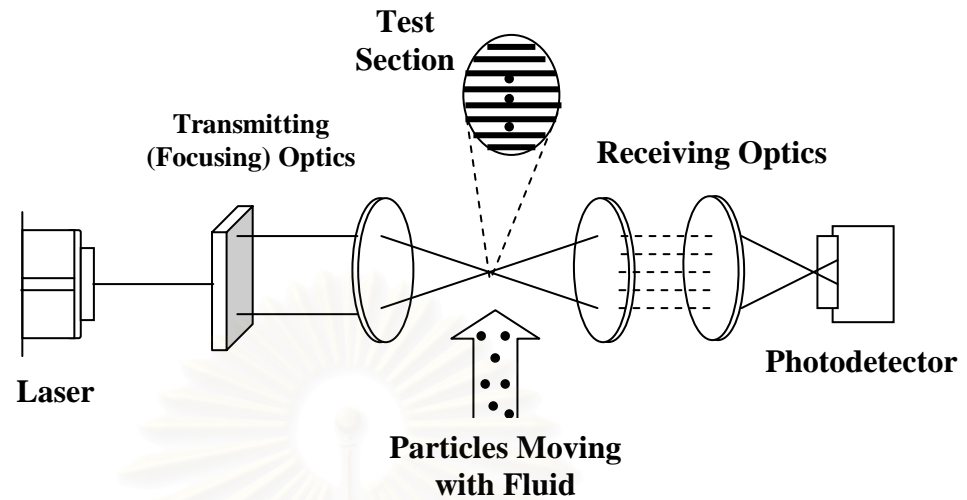


Figure 5.3 Typical optical setup of LDA instrument

5.4 Phase Doppler Anemometer (PDA)

The phase-Doppler technique is a well established and widely used technique for measurement of size and velocity of atomized droplets dispersing in two-phase flow by using two or more photodetectors. The phase shift of the light scattered by refraction or reflection from the two intersecting laser beams is used to obtain the particle size. Figure 5.4 illustrates the essential optical configuration of a PDA.

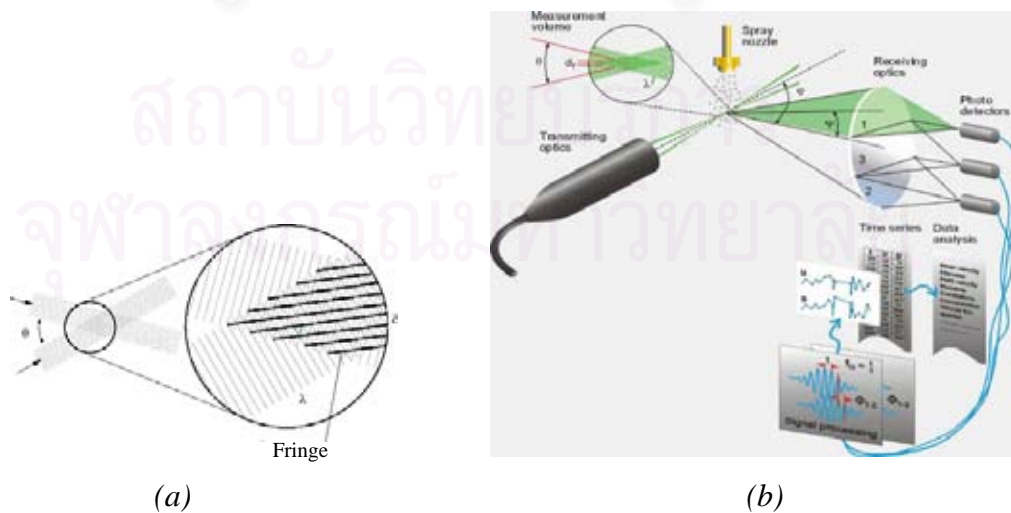


Figure 5.4a A scheme of the optical probe with fringes

5.4b PDA Configuration [20]

For two photodetectors placed at a certain off-axis angle (φ) and placed symmetrically with respect to the bisector plane at the elevation angles ($\pm\psi$), one obtains signals with phase difference ($\Delta\phi$) which could be estimated from

$$\Delta\phi = (2\pi D n_m / \lambda_e) \Phi \quad (5.7)$$

where D is droplet diameter, n_m is refractive index of surrounding medium and λ_e is the laser wavelength. The parameter Φ depends on the scattering mode.

For reflection

$$\Phi = \sqrt{2} [(1 + \sin\theta \sin\psi - \cos\theta \cos\psi \cos\varphi)^{1/2} - (1 - \sin\theta \sin\psi - \cos\theta \cos\psi \cos\varphi)^{1/2}] \quad (5.8)$$

And for 1st order refraction

$$\Phi = 2 \left\{ \left[1 + m^2 - \sqrt{2} m (1 + \sin\theta \sin\psi + \cos\theta \cos\psi \cos\varphi)^{1/2} \right]^{1/2} - \left[1 + m^2 - \sqrt{2} m (1 - \sin\theta \sin\psi + \cos\theta \cos\psi \cos\varphi)^{1/2} \right]^{1/2} \right\} \quad (5.9)$$

where $m = n_d / n_m$, the ratio of the refractive index of the particle (n_d) to that of the surrounding medium (n_m), has been used for convenience and 2θ represents the angle between the two incident beams.

Even if the absolute phase cannot be measured but the phase difference between the two detectors ($\Delta\phi$) is measurable and given by a law where only the particle diameter is unknown. The measure of the phase difference between two detectors is then a measure of the particle size.

For a standard PDA, with the notation introduced in Figure 5.5

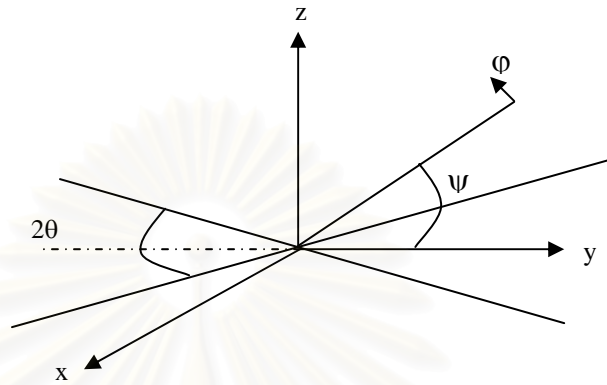


Figure 5.5 The definition of the scattering angle for a standard configuration

by recording the band-pass filtered Doppler signals from the two photodetectors, the phase $\Delta\phi$ is determined from the time lag (Δt) between the two signals as indicated in Figure 5.6

$$\Delta\phi = 2\pi \frac{\Delta t}{T} \quad (5.10)$$

where T is the time of one cycle of the signal. So the particle diameter can be determined from the following equation,

$$D = \frac{\lambda}{2\pi m_m} \frac{1}{\Phi} \Delta\phi \quad (5.11)$$

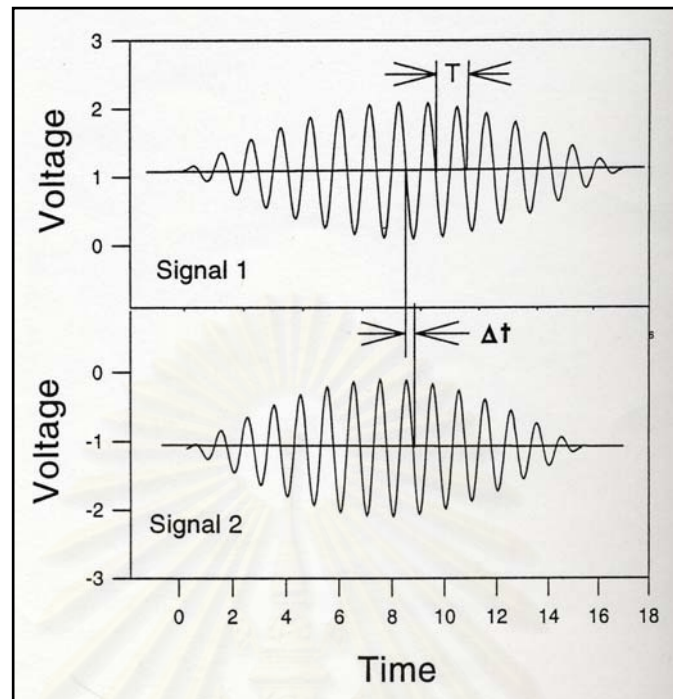


Figure 5.6 Determination of phase shift from two band-pass filtered Doppler signal [19]

From equation (5.10) and Figure 5.6, it follows that only a phase shift between zero and 2π can be distinguished with a two detector PDA system, which limits the measurable particles size range for a given optical configuration. Therefore, three detectors system is also used in which two-phase differences are obtained from detector pairs having different spacing as shown in Figure 5.7. This method enables one to extend the measurable particle size range while maintaining the resolution of the measurement.

For small particles, diffraction represents an especially important contribution to the light scattering that may affect and disturb the phase measurement. Therefore, the more general Mie theory has to also be applied to determine the scattering characteristics for a particle of any given size [19]. However, Mie theory is not used because of the diffraction, but to more accurately take into account complex phenomena as at rainbow or due to the mixing of several kind of interaction and for the small size of particle where the geometrical optics is not as good as for the big

ones. The Mie theory relies on the direct solution of Maxwell's equation for the case of the scattering of a plane light wave by a homogeneous spherical particle for arbitrary size and refractive index. In order to calculate the scattered field of a PDA system, it is necessary to add the contributions of the two incident beams and the average over the aperture of the receiving optics configurations. To allow for the influence of the Gaussian beam, the generalized Lorenz-Mie theory (GLMT) has also been recently applied to optimize PDA system [19].

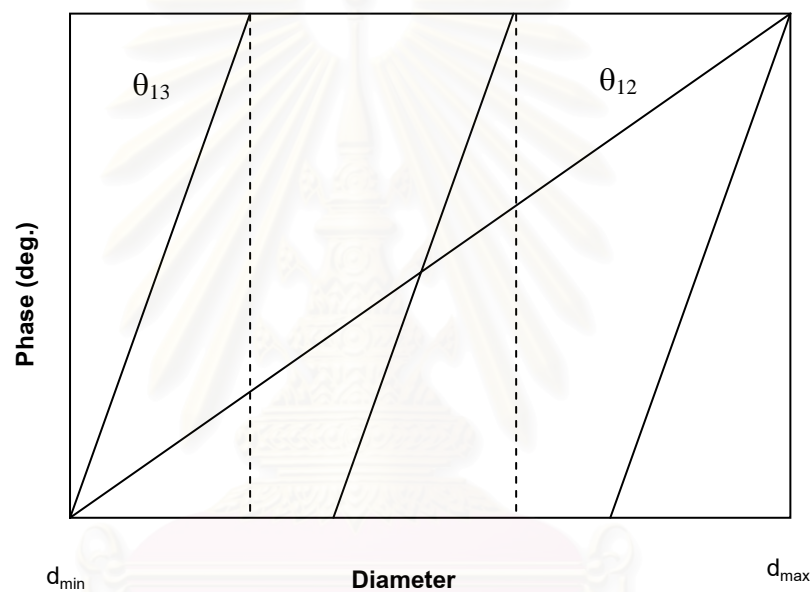


Figure 5.7 Representative response functions for a PDA system using three detectors

สถาบันวิทยบริการ
จุฬาลงกรณ์มหาวิทยาลัย

CHAPTER 6

RESULTS AND DISCUSSION

This chapter is devoted to reporting and discussing the experimental results. It mainly covers the dependence of spray characteristics on experimental parameters. The homemade Phase Doppler Anemometer developed at CEPT, Chulalongkorn University, has been used for measurement of a water spray, and the measurement results are discussed in order to obtain a fundamental understanding of the PDA. Optic techniques which are needed for measuring the characteristics of liquid droplets in a spray have also been described.

The spray characteristics observed are the local drop size distribution and the velocity profile. The spray produced by the two-fluid atomizer has also been investigated for a comparison of mixture of palm oil and diesel and commercial diesel sprays. The results are discussed for two issues, the spray drop size distribution and the velocity profiles. In the first part the Sauter Mean Diameter (D_{32}) which is useful for mass transfer reaction in combustion is examined. While the mean diameter (D_{10}) which is easy to obtain from the drop size distribution, is also conducted.

6.1 Measurement by the Homemade PDA

The homemade Phase Doppler Anemometer was developed by a preceding researcher, Tanonchai Boonnathee, in 2003. It was comprehensively verified that it can be used to measure the droplet size distribution generated by a two-fluid atomizer and an ultrasonic nozzle. However, for liquid fuels no experiments have been conducted yet. Due to the limitation of the lab, the atomization of flammable fuel could not be performed safely. Therefore, this part shows the results of a water spray produced by a two-fluid atomizer with the homemade PDA for the sake of re-verification.

The mean velocities of water spray with various injection pressures is shown in Table 6.1. This is to confirm that the developed equipment could provide reliable measurement results. Based on the present verification, it could only measure the droplet velocity correctly in some certain range of 5 to 20 m/sec because the optic materials were installed in an un-controllable atmosphere. However, droplet velocity measures also depend on optic parameters (see Chapter 3).

Based on the experimental results shown in Table 6.1, the drop velocity of water spray increases as the air injection pressure rises. It should be noted that there is some error due to the limitations of the developed equipment and adjustments that were needed for this work. The home-made PDA could provide sufficiently reliable measurements based on the re-verification results.

Table 6.1 Mean velocity of water spray measured by homemade PDA

Spray Injection Pressure (bar)	Mean velocity at 7 cm. (m/sec)
0.5	6.55
1	14.72
1.5	20.13

สถาบันวิทยบริการ
จุฬาลงกรณ์มหาวิทยาลัย

6.2 Stages of Atomization

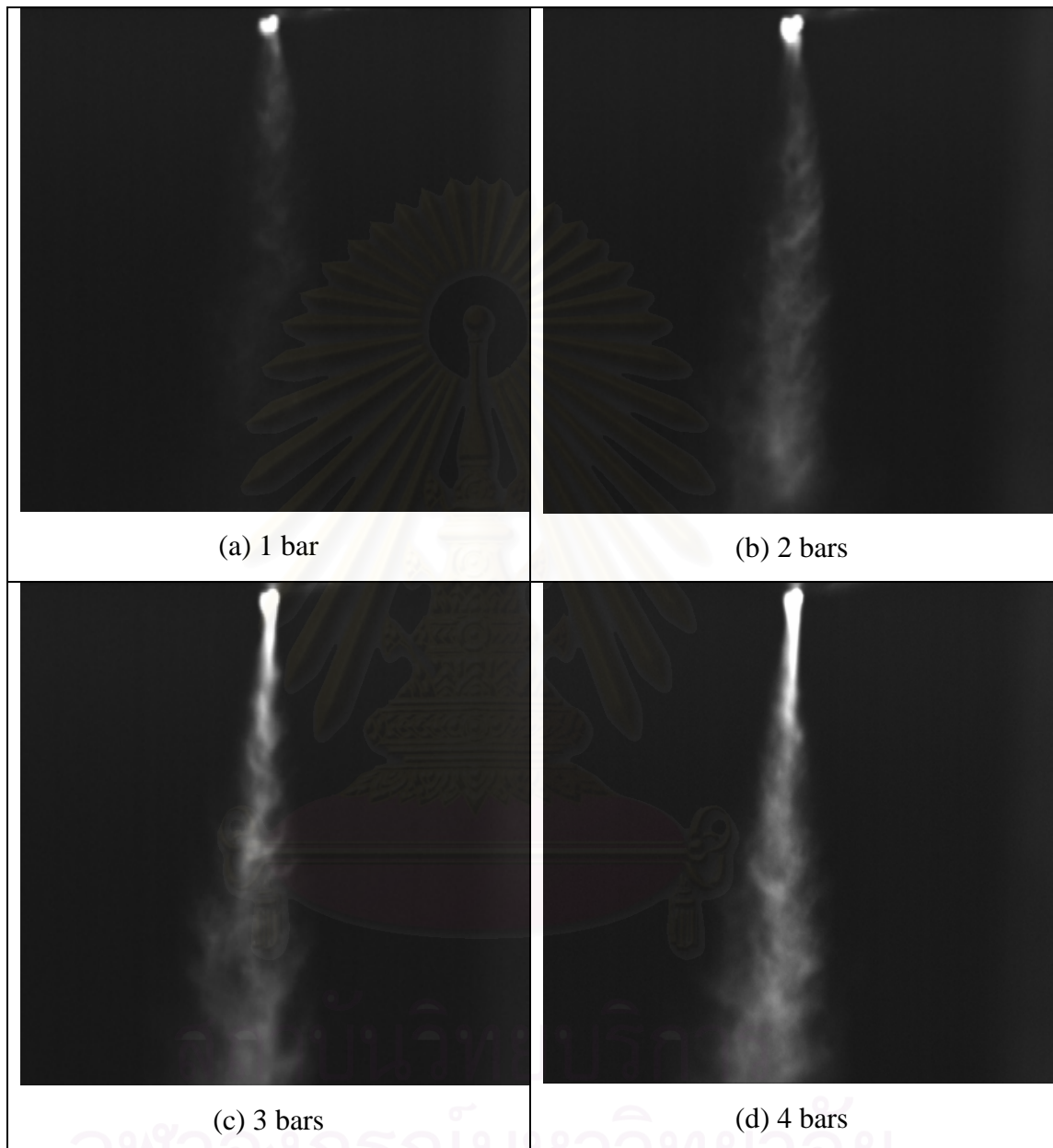


Figure 6.1 Sprays development by an external-mixed two-fluid atomizer

Figure 6.1 shows pictures taken by a Charge-Coupled Devices (CCD) camera to display the development of a fuel spray generated by an external-mixed two-fluid atomizer. The injection pressure applied to diesel fuel was varied from 1 to 4 bars. At the beginning, a diluted spray was emerging from an orifice after slightly opening the

valve at 1 bar as seen in Figure 6.1(a). When the valve is opened further, more and more liquid was leaving the nozzle as seen in Figure 6.1 (b), (c) and (d). Moreover, further from the nozzle tip the spray becomes more diluted. That is attributed to the evaporation of drops and the air entrainment induced by some drops out of the spray. In addition, the spray angle is not so much different with increasing air injection pressure and very small, which is related to the explanation of Lefebvre [17] given before.

6.3 Discharge Coefficient

Lefebvre [17] explained one important characteristic of an atomizing nozzle, namely the discharge coefficient. This characteristic is governed partly by the pressure losses incurred in the nozzle flow passages and also by the extent to which the liquid flowing through the final discharge orifice makes full use of the available flow area. That means that the discharge coefficient can be used as an indicator for the performance of the nozzle; a high discharge coefficient means a high mass flux throughout the orifice.

Discharge coefficients (C_d) of the atomizer for diesel and palm oil mixtures are shown in Figure 6.2. The results show that discharge coefficients are generally constant with increasing pressure. The discharge coefficient of diesel is higher than that of its blends and neat palm oil. The average value is in the range of 0.05-0.1 while the maximum discharge coefficient is 0.803 (see Chapter3). This can be explained by the definition of the discharge coefficient which it is the ratio of actual to theoretical flow. Hence, in this case the two-fluid atomizer can discharge the liquid with a mass flow rate of only 5-10 per cent of the theoretical amount.

Figure 6.2 suggests that for a certain type of liquid fuel, the air injection pressure provides no significant effect on C_d . It should be noted that most of the spray is air therefore C_d is quite low. On the other hand, Figure 6.3 shows that at air injection pressure of 1 bar, the ratio of cooking oil added to the blended mixture exerts a strong effect on the C_d . It is clearly observed that the more the amount of cooking oil, the less the C_d . This is attributed to the fact that the viscosity of a blended

fuel affects C_d strongly. It can also be seen in Figure 6.4 that the amounts of palm oil influences the kinematic viscosity of the blended fuel.

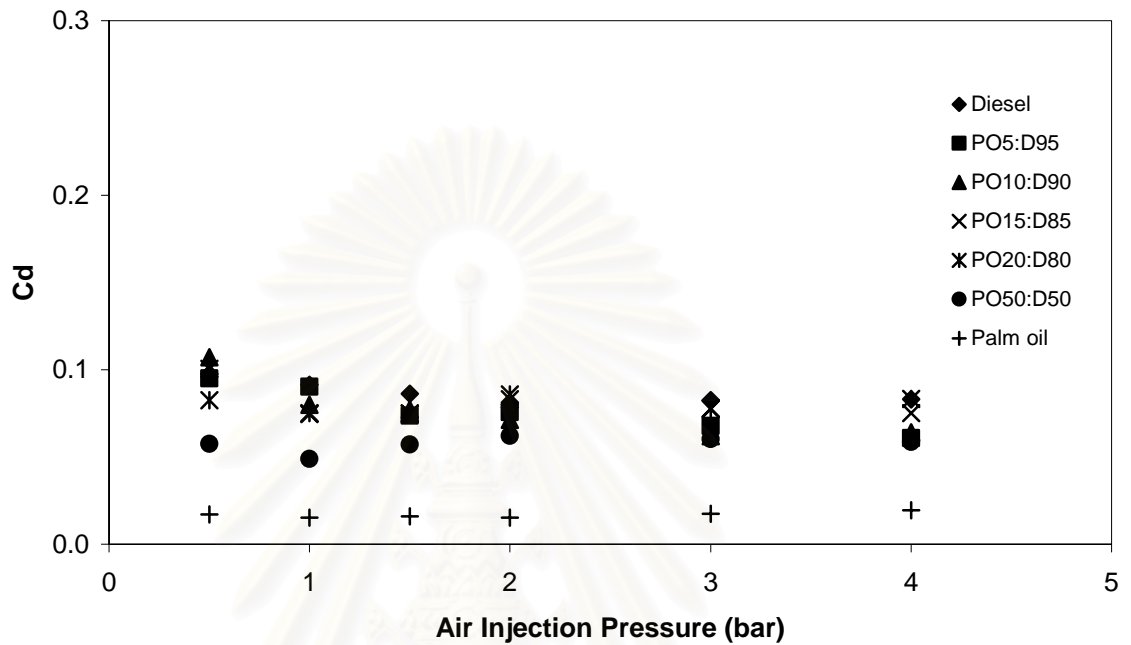


Figure 6.2 Effect of injection pressure on discharge coefficient of two-fluid atomizer

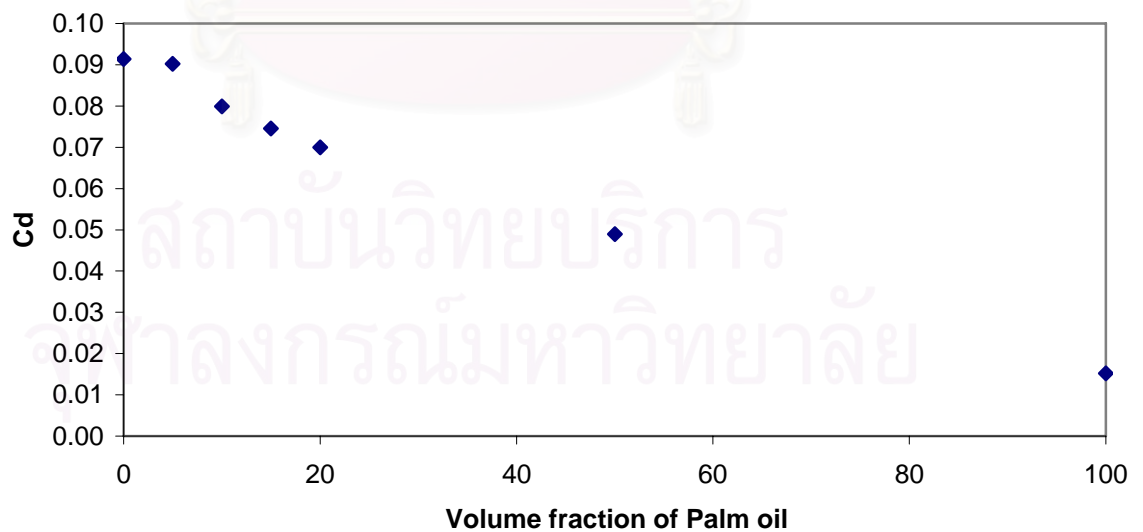


Figure 6.3 Effect of volume ratio of palm oil to diesel on discharge coefficients of fuels at 1 bar air injection pressure

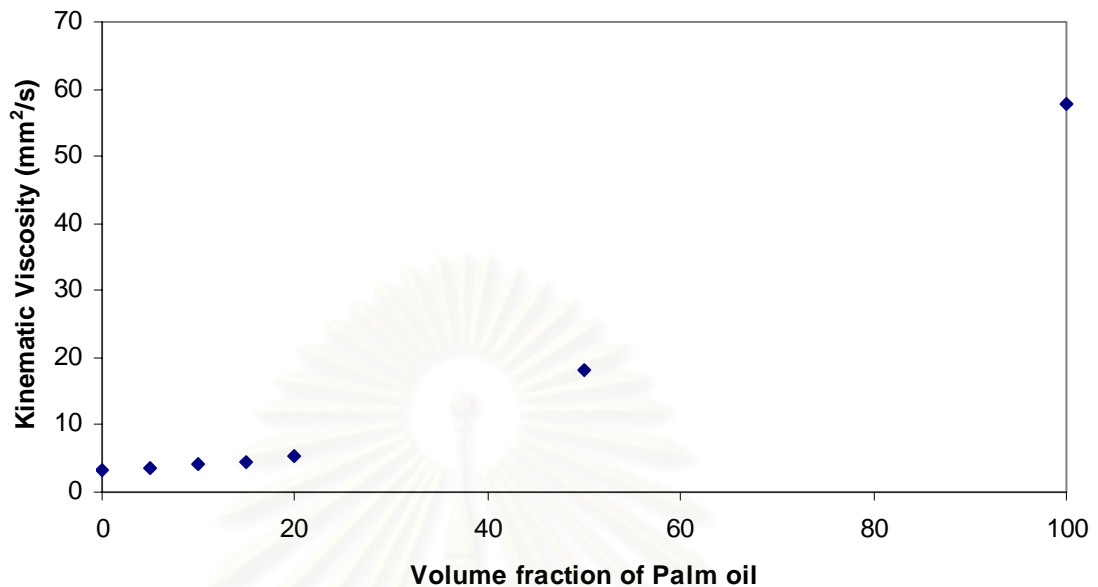


Figure 6.4 Effect of volume ratio of palm oil on Kinematic viscosity of blended fuel

6.4 Size and Velocity Measurement by a Commercial PDA

The size distribution of the spray generally exhibits two different mean diameters. On the one hand there is the normal mean diameter, D_{10} , from which it is easy to see the tendency of the distribution and which can easily be used to compare previous results with new experiments. On the other hand there is the Sauter Mean Diameter (SMD), D_{32} , which is useful to study mass transfer in combustion and evaporation because the SMD is the diameter of the drop whose ratio of volume to surface area is the same as that of the entire spray. Therefore, the SMD is the only mean diameter which can properly indicate the fineness of a spray from a combustion viewpoint. The velocity profile will be shown in average axial velocity of drops. Moreover, only spherical drops were taken into account. The commercial program for the PDA can indicate the shape of those drops. This causes a decrease in error from measurements.

It is necessary to show that the spray system provides a steady state over time. Table 6.2 shows the arithmetic mean diameter of the spray at different measurement points. All drops in the same measurement point will be divided into three parts from

the first to the last drop. It shows that the mean diameter for these three parts gives significantly the same value. It can be concluded that the spray system produces steady state atomization.

Table 6.2 Arithmetic mean diameter of the spray at different measuring points

Liquid fuel	1 st period	2 nd period	3 rd period
PO20:D80 at 5 cm, center	10.729	10.775	10.930
PO20:D80 at 5 cm, -2 mm	10.958	10.387	10.974
PO20:D80 at 5 cm, 2 mm	9.810	9.846	9.821
PO20:D80 at 7 cm, center	13.582	13.188	13.291

In the following parts PO20:D80 is used as an example of a liquid fuel spray to show the effects on the size distribution and the velocity profile. Also, 20 per cent of biofuel blended with diesel represents a good balance of cost, emissions, cold weather performance, materials compatibility, and solvency [4]. However, all blended mixtures have similar effect on the size distribution and velocity profile.

Before considering the influence on the local mean diameter, Table 6.3 shows representative drop diameter. Considering the small drops on the basis of $D_{0.1}$, it is found that their values of PO20:D80 and PO50:D50 sprays are slightly larger than diesel spray, implying that the diesel spray has smaller drops. When big drops are considered, it is seen that $D_{0.9}$ of diesel, PO20:D80 and PO50:D50 indicating larger drops in mixture with palm oil. Moreover, the lower $D_{0.5}$ also indicates that diesel sprays are finer than mixture with palm oil fuel at this pressure.

Table 6.3 Size distribution parameters of diesel, PO20:D80, and PO50:D50 sprays ($P_{inj} = 1$ bar, $z = 5$ cm, center of spray)

	$D_{0.1}$ (μm)	$D_{0.5}$ (μm)	$D_{0.9}$ (μm)	D_{32} (μm)	Span
Diesel	10.8	18.6	30	16.55	1.03
PO20:D80	12.1	21.2	40.4	19.19	1.33
PO50:D50	12.7	26.1	48.9	24.69	1.39

➤ The effect of air injection pressure

The sensitivity of the droplet diameter with respect to the air injection pressure has been studied because the air injection is the beginning of the atomization process. The limitations for air injection of the two-fluid atomizer in this research are 0.47 bars to 4 bars (Pawin Engineering Co., Ltd.). It has been studied in the range of 0.5, 1, 1.5, 2, 3, and 4 bars. The liquid is delivered to the atomizer by gravity through a medical syringe, therefore the mass flow rate of the spray depends only on the air injection pressure.

Figure 6.5 shows the particle diameters D_{10} versus the injection pressure at the 0 mm and ± 2 mm around the center of the spray. For the injection pressure range of 0.5-4 bars, a first observation is that the mean diameter (D_{10}) is essentially constant in the range 10-12 micron. The droplet diameter slightly decreases when the injection pressure is increased [21]. It can be confirmed by the series of Figure 6.6 that the mean diameter of droplets is stable. Figure 6.6 (a) displays the size distribution corresponding to an injection pressure equal to 0.5 bar while Figure 6.6 (b) and (c) display the size distribution corresponding to the injection pressure of 1 and 4 bars respectively. These figures show that the size distribution of the mean diameter is essentially independent of the injection pressure as the main peak in those figures are at about 11 μm but at the high pressure the size of droplets are a bit smaller. However, the size distribution at higher injection pressure gives a more uniform size as indicated by the span in Figure 6.6.

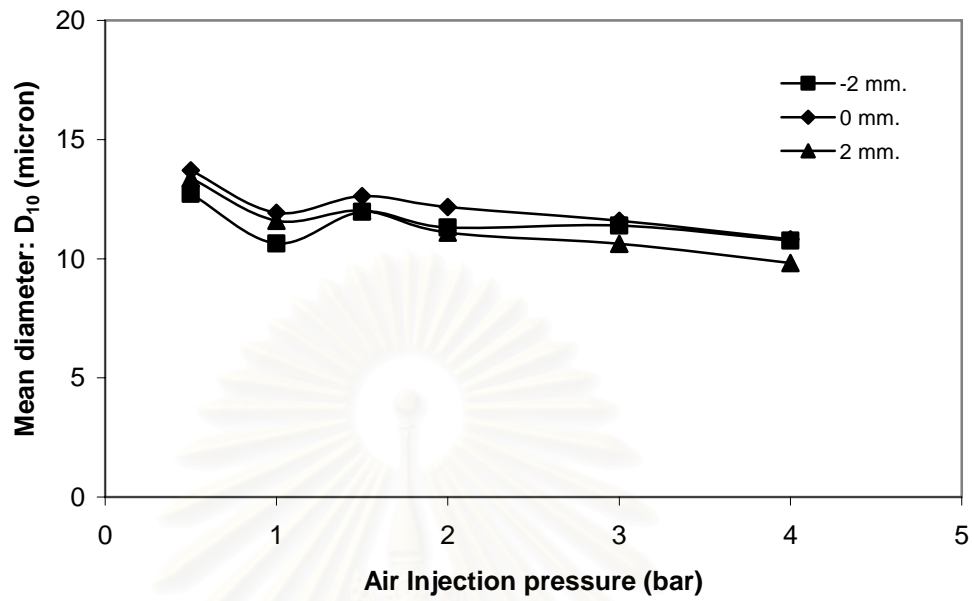
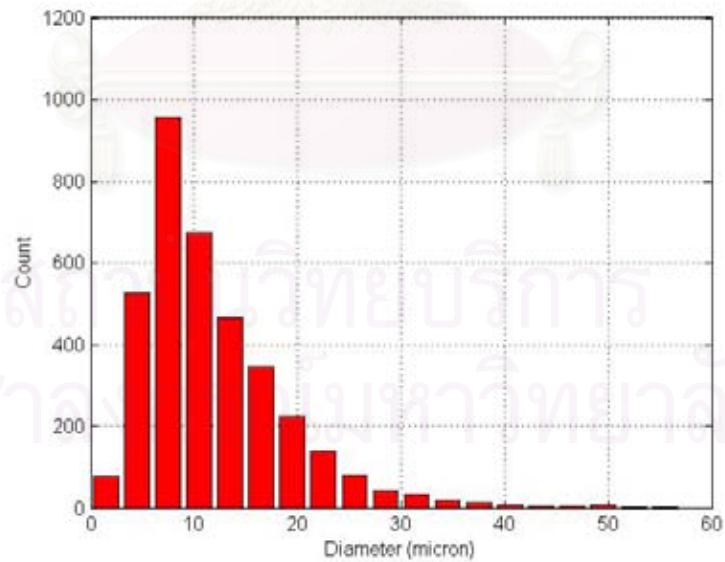
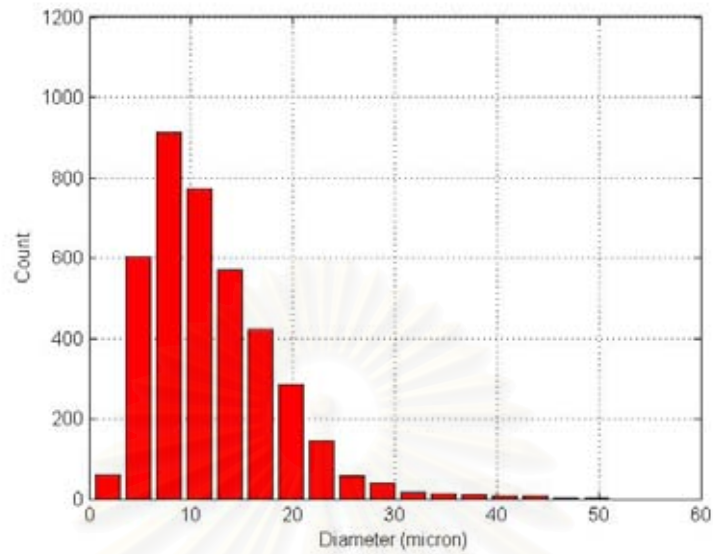


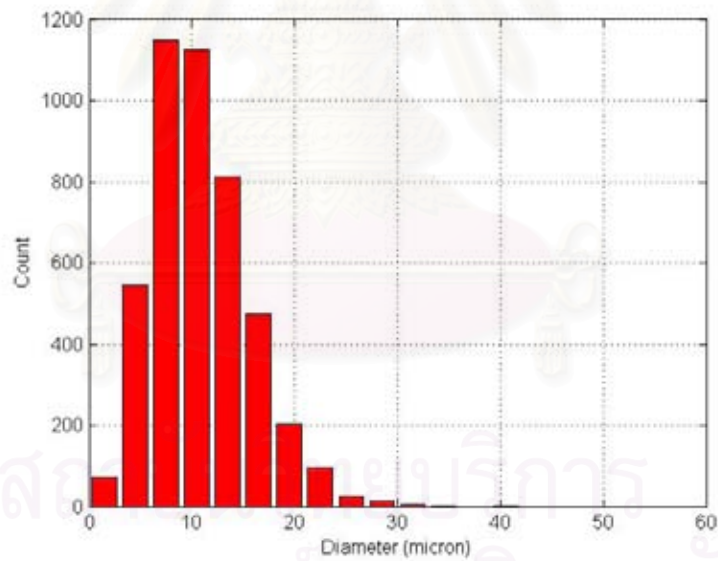
Figure 6.5 Mean diameter (D_{10}) versus the injection pressure for PO20:D80 spray at 5 cm away from atomizer tip



(a) span = 1.86



(b) $span = 1.33$



(c) $span = 0.87$

Figure 6.6 Droplet size distribution of PO20:D80 spray.

The injection pressure is equal to
(a) 0.5 bar (b) 1 bar and (c) 4 bars

The effect of air injection pressure on the span of the drop size distribution is also shown in Figure 6.7. It clearly shows that the span decreases when the air

injection pressure increases which means high air injection pressure leads to more uniform drops in the spray.

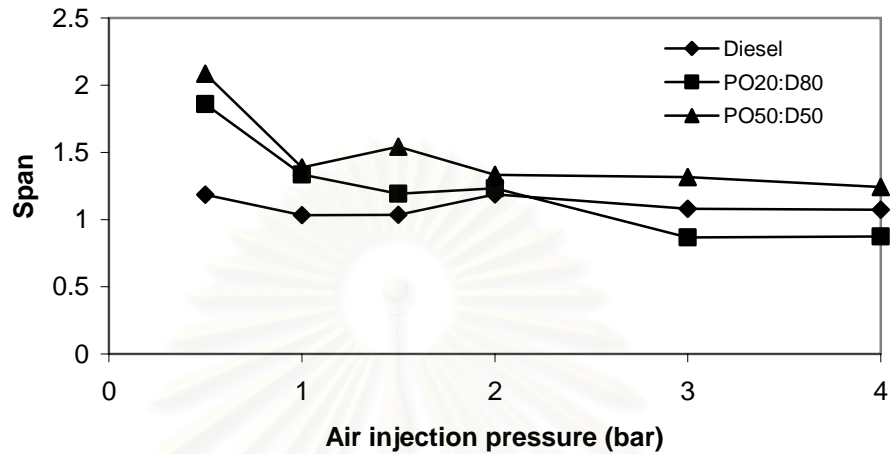


Figure 6.7 Effect of air injection pressure on span of drop size distribution

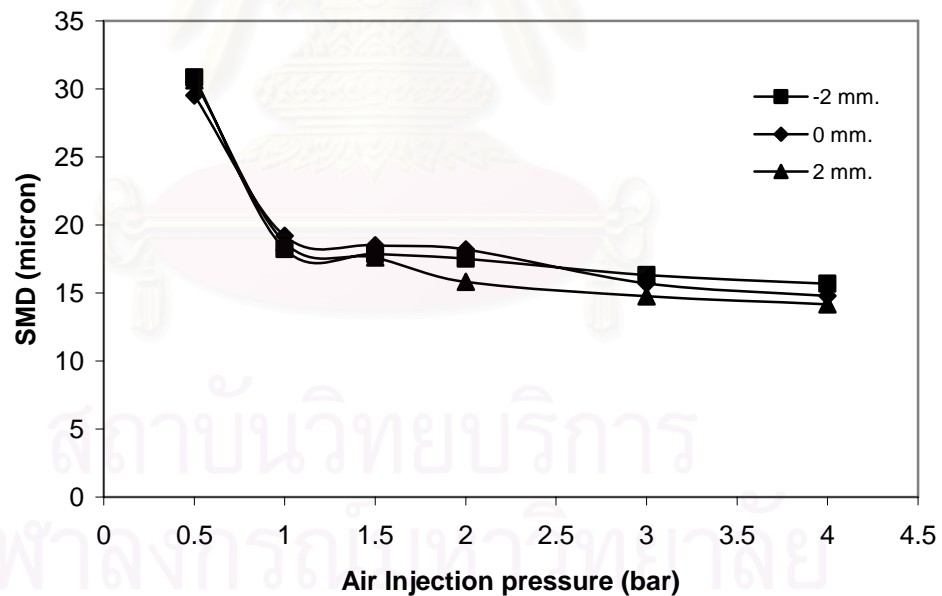


Figure 6.8 Sauter Mean Diameter (D_{32}) versus the injection pressure for PO20:D80 spray at 5 cm away from nozzle tip

In case of the Sauter Mean Diameter (D_{32}), the low injection pressure clearly affects the droplet sizes as shown in Figure 6.8. The low injection pressure in the

range of 0.5-1 bars results in the generation of large droplets. This is attributable to the fact that the viscosity of the blended fuel dominates the size of droplets generated at low injection pressure [22]. Injection pressures higher than 1 bar have a slight influence on the droplet diameter as shown in the graph. It can be concluded that the Sauter Mean Diameter of a spray generated by the two-fluid atomizer would distinguishably decrease with the increasing air injection pressure up to 1 bar. The further injection pressure would not result in a significant decrease in droplet size.

Regarding the effect of injection pressure to velocity profile, Figure 6.9 shows that the mean axial velocity is generally increased with increasing injection pressure. It was explained before that most of the spray is air which has more momentum than fuel. Therefore, the injection pressure influences the velocity.

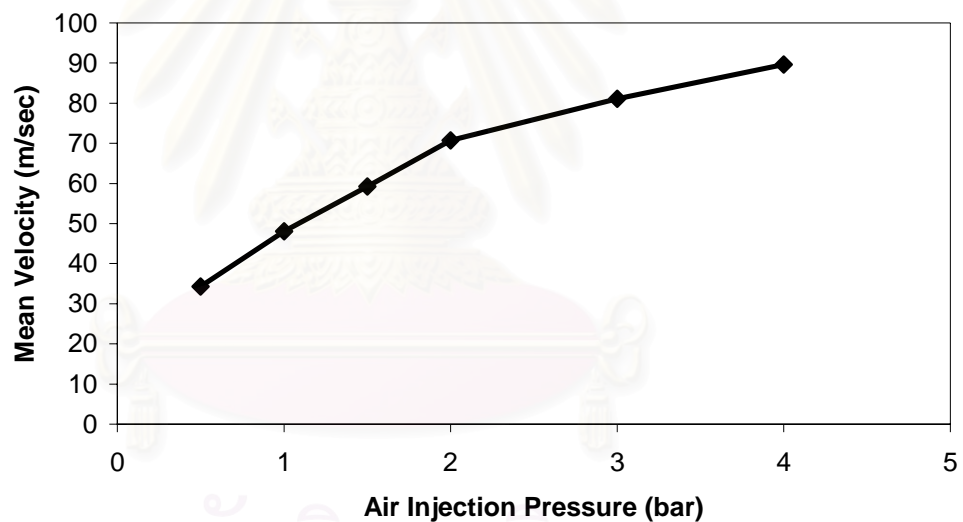


Figure 6.9 Velocity profile of PO20:D80 on the center region of spray

(z = 5 cm)

➤ The effect of traveling distance

Once the atomization process is completed, there are three main factors that influence the change of droplet size distribution. They are: the effect of evaporation, the effect of spray dispersion and the effect of droplet acceleration (or deceleration) [23].

In this work, measurements were performed at different traveling distances, 5 and 7 cm from the nozzle tip. Very close to the atomizer tip a very dense spray is found of which cannot be used to measure the size and velocity correctly because the tool could not detect all the drops. However, very far from the atomizer tip, there are too many droplets which are strongly disturbed by evaporation and coalescence of drops, so measurements too far from the atomizer tip do not provide the correct spray characteristics.

Regarding to mean droplet size along downstream, it is shown clearly in Figures 6.10 and 6.11 that the traveling distance has a significant influence on the drop size distribution. Figure 6.10 shows the mean diameter against the radial distance at two traveling distances, at 5 and 7 cm from the atomizer tip. The drop sizes at the longer traveling distance are larger than those at the short distance. The parameter accountable for this change would be the evaporation of small droplets and their drop deceleration. It should be noted that droplet deceleration of smaller drops with lower momentum by air drag could be observed visually in the experiments of Chin et al [23].

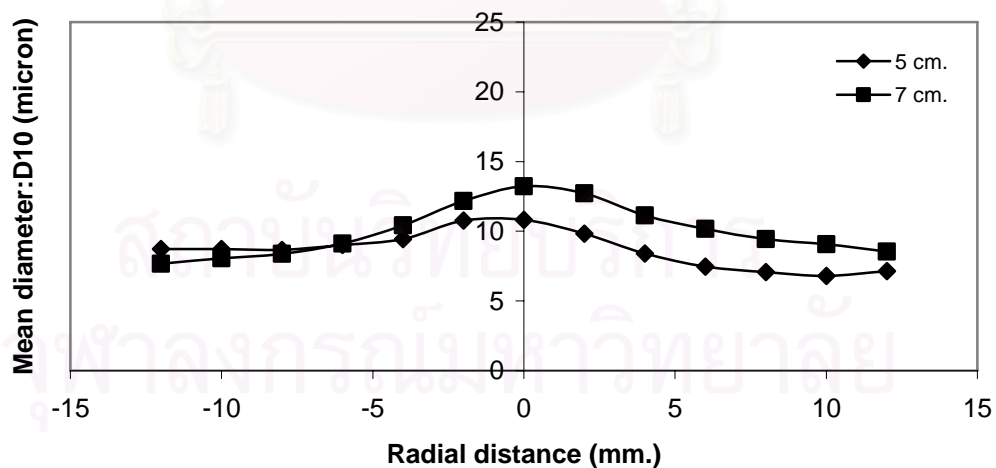


*Figure 6.10 the effect of downstream distance on spray for Mean Diameter (D_{10})
($PO_{20}:D_{80}$, $P_{inj} = 4$ bar)*

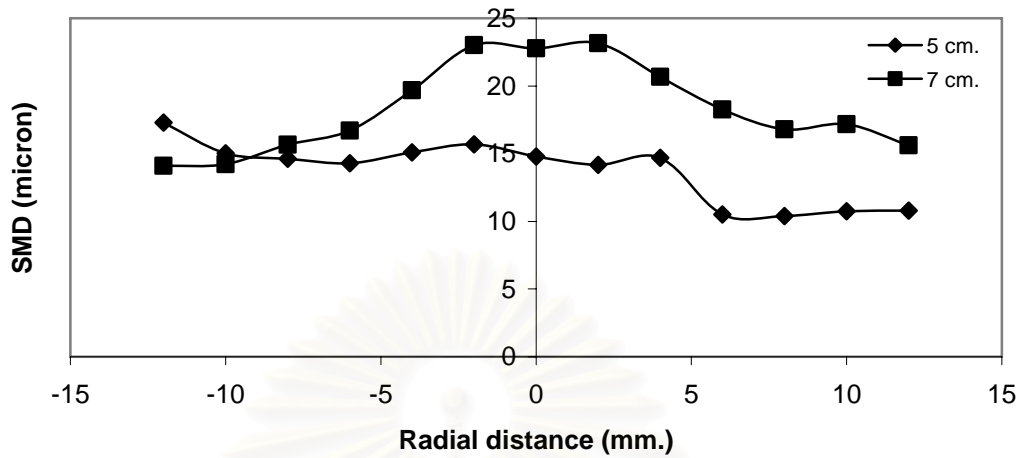


Figure 6.11 the effect of downstream distance on spray for Sauter Mean Diameter (D_{32}) (PO20:D80, $P_{inj} = 4$ bar)

In Figure 6.11 the Sauter Mean Diameter of PO20:D80 spray is shown along radial distance and at 5 and 7 cm away from atomizer tip. The larger drops are found at long traveling distance for the same reasons as is the case for the mean diameter (D_{10}). However, movement of small drops into the inner region of the spray by air entrainment also causes for larger drop sizes at the edge of the spray as seen in Figure 6.11, which shows the influence of the radial distance on the distribution. Thus, it can be concluded that the two-fluid spray drops are not stable along downstream distance but they are stable along radial distance except at the edge. However, size distribution at 5 cm in Figure 6.11 does not seem to be symmetric. In any case, it can be confirmed with the size distribution of PO50:D50 in Figure 6.12 that it is acceptably symmetric along the radial distance at both measurement points, 5 and 7 cm. Thus, it can be concluded that in some experiments there is an error because the effect of air emission at the outermost of the spray emits some drops out of probe volume.

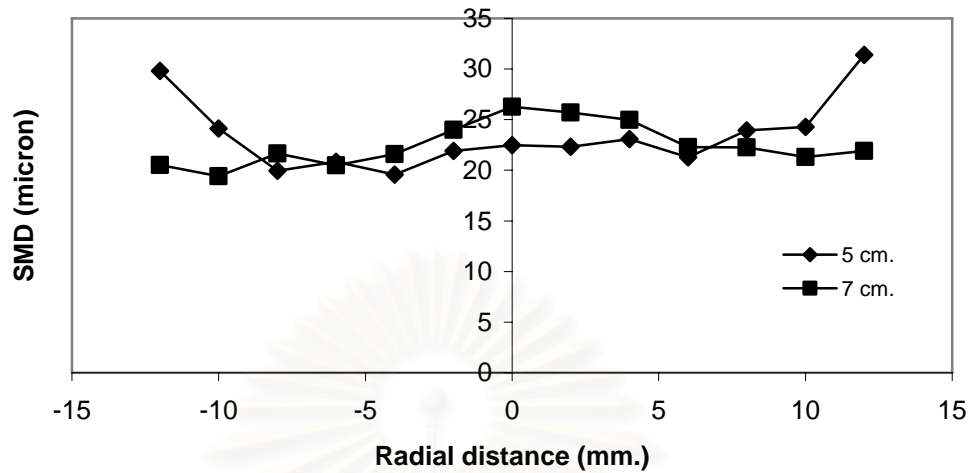
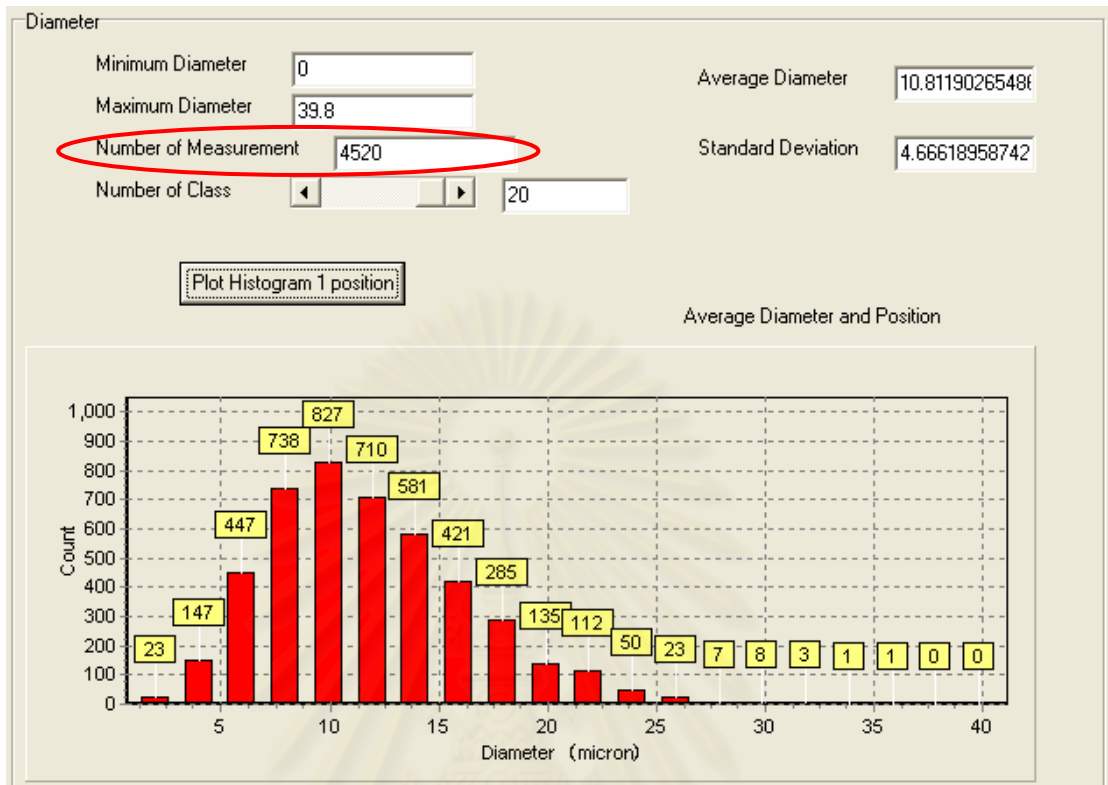


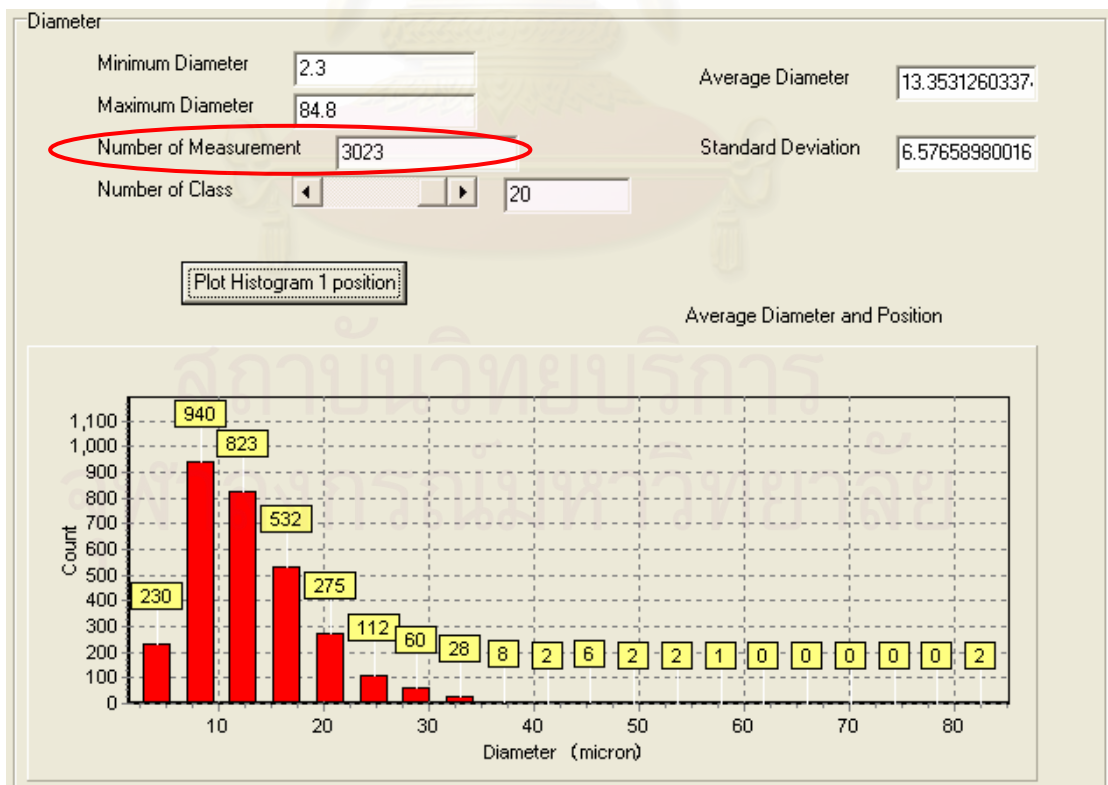
Figure 6.12 the effect of downstream distance on spray for Sauter Mean Diameter (D_{32})(PO50:D50, $P_{inj} = 2 \text{ bar}$)

The drop evaporation is also confirmed by the measurements of the number of drops along traveling distance. The number of drops at longer traveling distance is less than at shorter distance. Figure 6.13 (a) and (b) show the windows of the drop size distribution with the necessary information. The amount of drops at 5 cm traveling distance in Figure 6.13 (a) is higher than the amount at 7 cm, which verifies that fuel droplets evaporate along the traveling distance. Due to evaporation of small drops, less small drops are taken into account in the calculation of the average diameter. The average diameter at 7 cm is higher than at 5 cm.

สถาบันวิทยบริการ
จุฬาลงกรณ์มหาวิทยาลัย



(a) 5 cm away from atomizer tip



(b) 7 cm away from atomizer tip

Figure 6.13 Drop size distribution of PO20:D80 with 4 bar injection pressure

The mean velocity of particles is shown in Figure 6.14 which shows clearly that the downstream distance influences the droplet velocity. The mean velocity of particles closer to atomizer tip is faster. The major cause for this is the loss of energy by drag force along the path of the drops. Therefore, more remarkable effects of the traveling distance on the droplet velocity distribution could be expected.

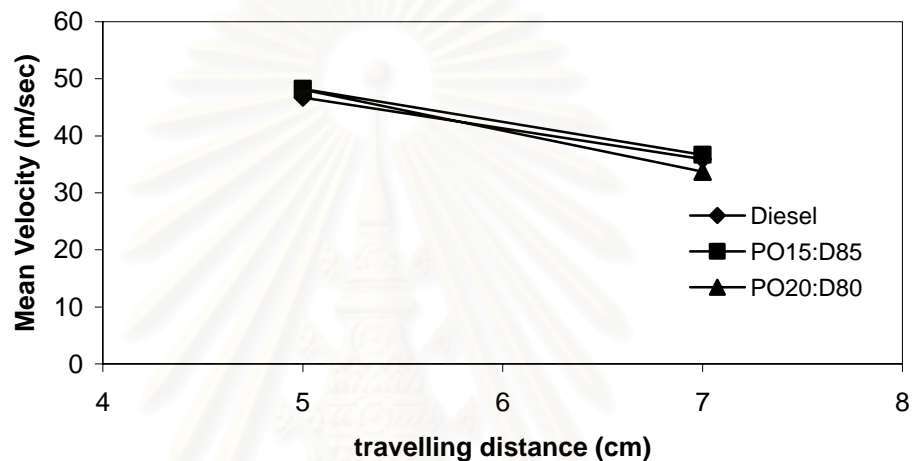


Figure 6.14 Mean velocity of drop along traveling distance

➤ Radial Distribution of the spray characteristics

The radial mean drop diameter is symmetric. Examples of such a behavior are presented in Figure 6.15 and Figure 6.16 for the mean diameter (D_{10}) and the Sauter Mean Diameter (D_{32}), respectively.

สถาบันวิทยบริการ
จุฬาลงกรณ์มหาวิทยาลัย

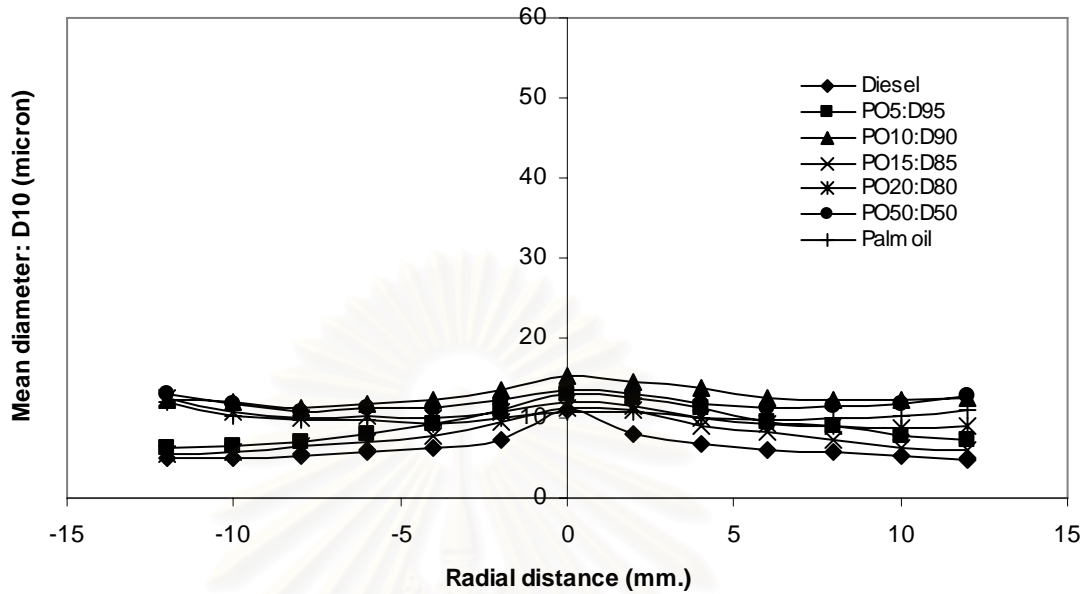


Figure 6.15 Radial distribution of Mean Diameter (D_{10}) at 5 cm away from atomizer tip ($P_{inj} = 1$ bar)

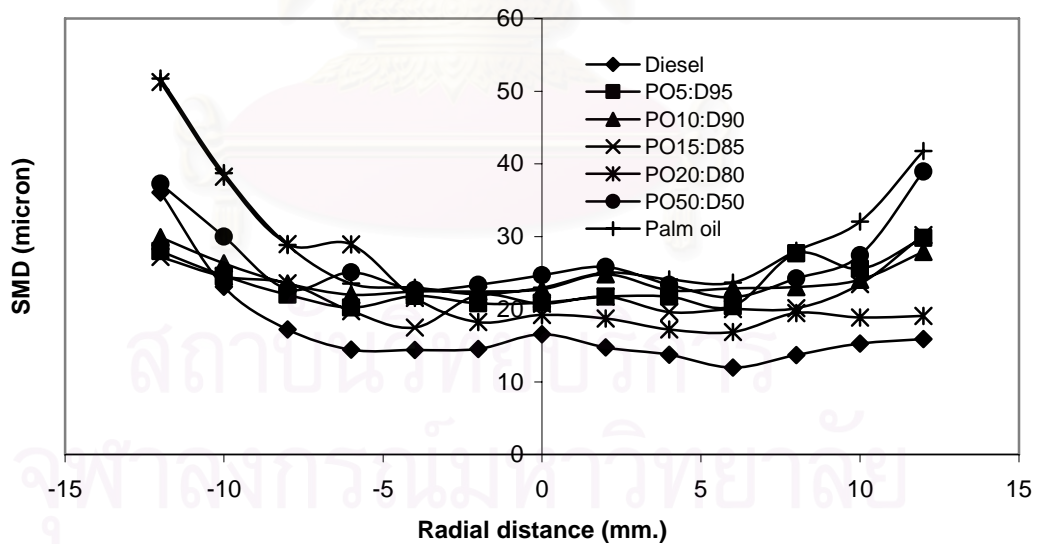


Figure 6.16 Radial distribution of Sauter Mean Diameter (D_{32}) at 5 cm. away from atomizer tip ($P_{inj} = 1$ bar)

In terms of the mean diameter (D_{10}), one may notice a symmetric distribution of the drop, the larger particles being located in the central region of the spray and the

smaller drop diameter at the edge. A slight increase is observed as can be seen in Figure 6.15. This behavior suggests that the increase of the mean drop diameter at some radial distance (about ± 10 mm, in these experiments) results from emissions of a few relatively big drops. This is due to the fact that the smaller drops are more easily induced into the center region of the spray by air entrainment. And also the evaporation of small drops at the edge is easier than larger drops; it is influenced for the statistic calculation. The radial distribution of the Sauter Mean Diameter, SMD, (D_{32}) in Figure 6.16 showed the same trend with D_{10} . It might be noticed that there are larger drops at the edge of the spray.

In cases of the velocity profile along radial distance, Figure 6.17 shows the mean velocity of diesel spray at 7 cm traveling distance with air injection pressure of 1 bar. It clearly shows that the highest velocity is found at the center region of spray as the distribution is symmetric. It behaves like a conventional jet flow [24].

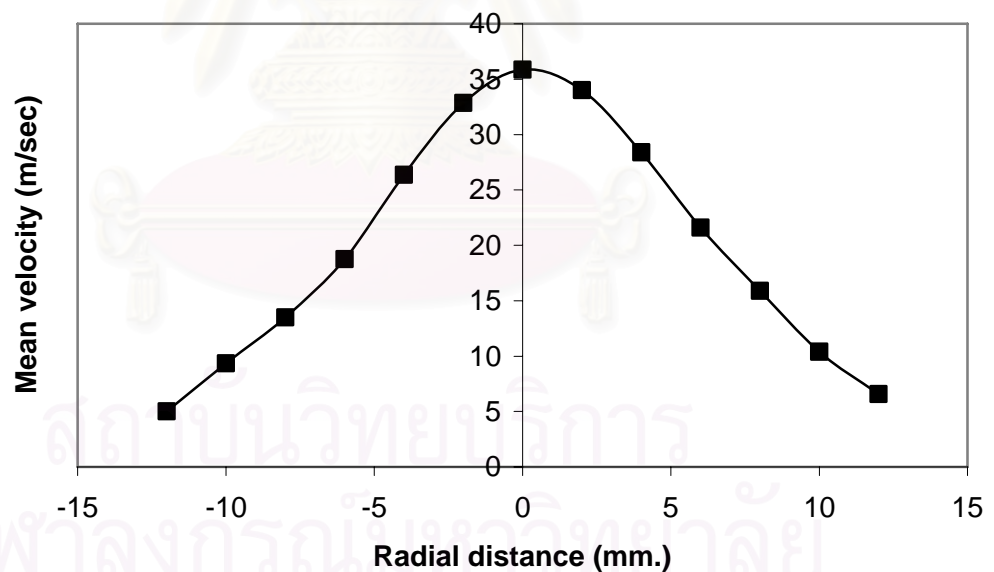


Figure 6.17 The velocity profile of spray at 7 cm. away from nozzle tip
(Diesel, $P_{inj} = 1$ bar)

➤ The effect of fuel properties

The mean diameter produced by the two-fluid atomizer is not only injection pressure dependent, but is also affected by density, viscosity and surface tension. In practice, it is impossible to change these parameters continuously and independently. Nevertheless, measurements have been performed for different products, which possess different physical properties (see Chapter 3).

Figure 6.18 shows the Sauter Mean Diameter against the radial distance to reveal the effect of different fuel compositions. Seven compositions have been studied: diesel, 5, 10, 15, 20, 50 and 100 percent by volume of palm oil mixed with diesel. As seen in Figure 6.18 the fuels which have very low viscosity (diesel) and very high viscosity (PO50:D50 and palm oil) exhibit obvious difference in their D_{32} distribution. The Sauter Mean Diameter of PO50:D50 and palm oil spray are larger than that of diesel. This could be implied that the higher the viscosity the more difficult the droplet generation. With gradual change in the composition leading to smaller difference in the fuel viscosity, gradual change of D_{32} could be observed.

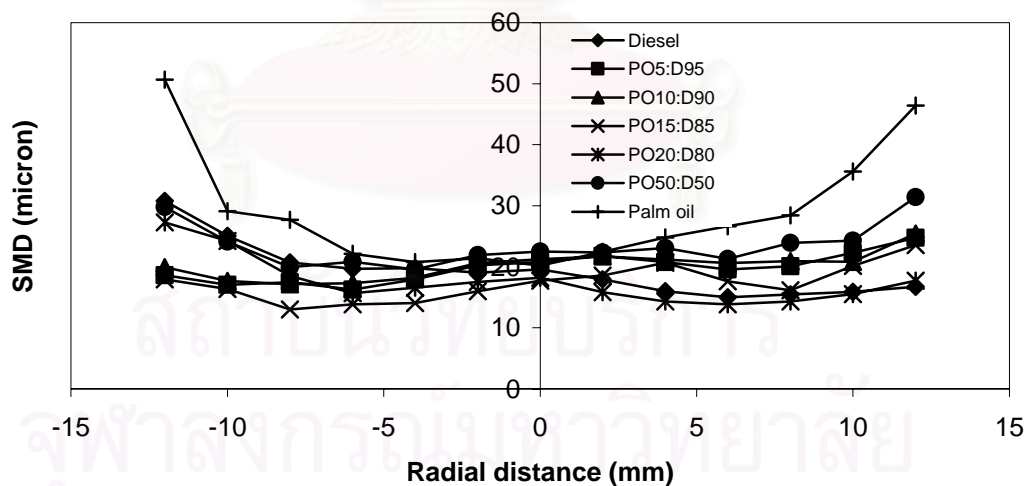


Figure 6.18 Parameters of drop size distribution of diesel, PO5:D95, PO10:D90, PO15:D85, PO20:D80, PO50:D50, and Palm oil ($P_{inj} = 2 \text{ bar}$, $z = 5 \text{ cm}$)

Nevertheless, there is no significant tendency on the mean axial velocity with different liquid fuels. The mean axial velocities at the same air injection pressure for

various liquid properties are the same. Figure 6.19 shows the mean axial velocity of diesel and the mixtures with air injection pressure of 1 bar, they are about the same at 50 m/sec. The possible reason for this is the particular characteristic of the two-fluid atomizer; the spray characteristics of a two-fluid air-assisted atomizer strongly depend on the interaction of gas and liquid inside the nozzle [25]. When the air is injected into the atomizer, it is not injected directly into the liquid, but it induces the liquid to be droplets. The velocity of the droplets we observed is the relative velocity between the liquid particle and the surrounding air. Likewise, it was discussed in the part about the discharge coefficient that most of the spray is air, so the droplets received strongly high momentum from the injection air. It can be concluded that droplet velocity depends on air injection pressure more than its properties. Therefore, this kind of atomizer gives the specific characteristic with respect to droplet velocity.

All types of blended oil give the same value for drop velocity if they are atomized at the same pressure. Figure 6.20 and 6.21 show velocity profiles of PO20:D80 with different air injection pressures at measuring points 5 and 7 cm away from nozzle tip, respectively.

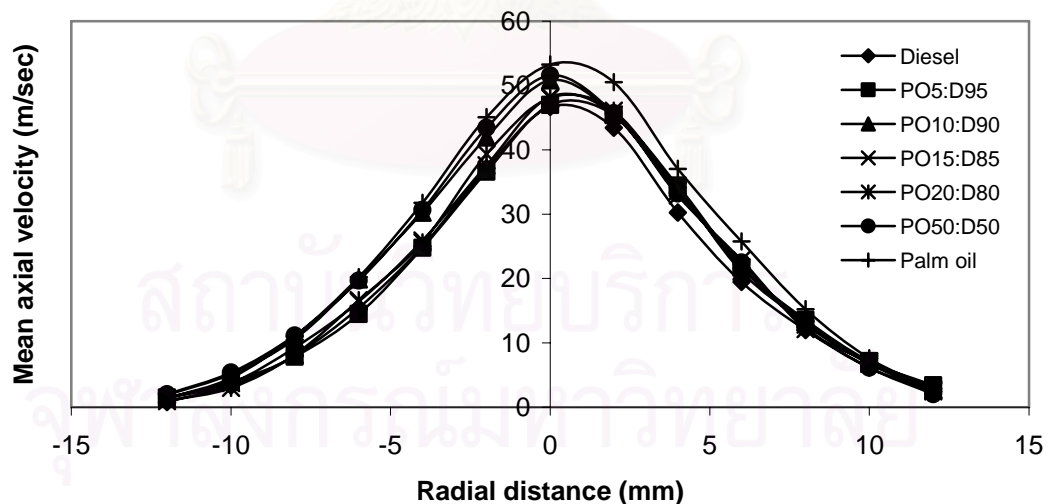


Figure 6.19 Velocity profiles of diesel and the mixtures spray at 5 cm away from tip

$$(P_{inj} = 1 \text{ bar})$$

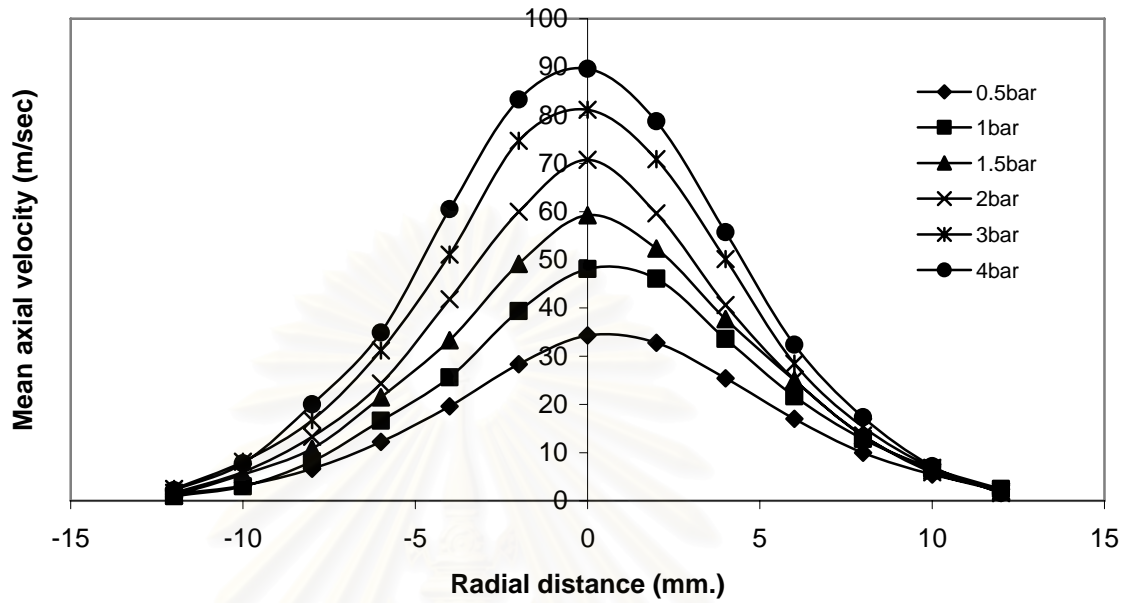


Figure 6.20 Axial mean velocity of PO20:D80 with different injection pressure at 5 cm. away from atomizer tip

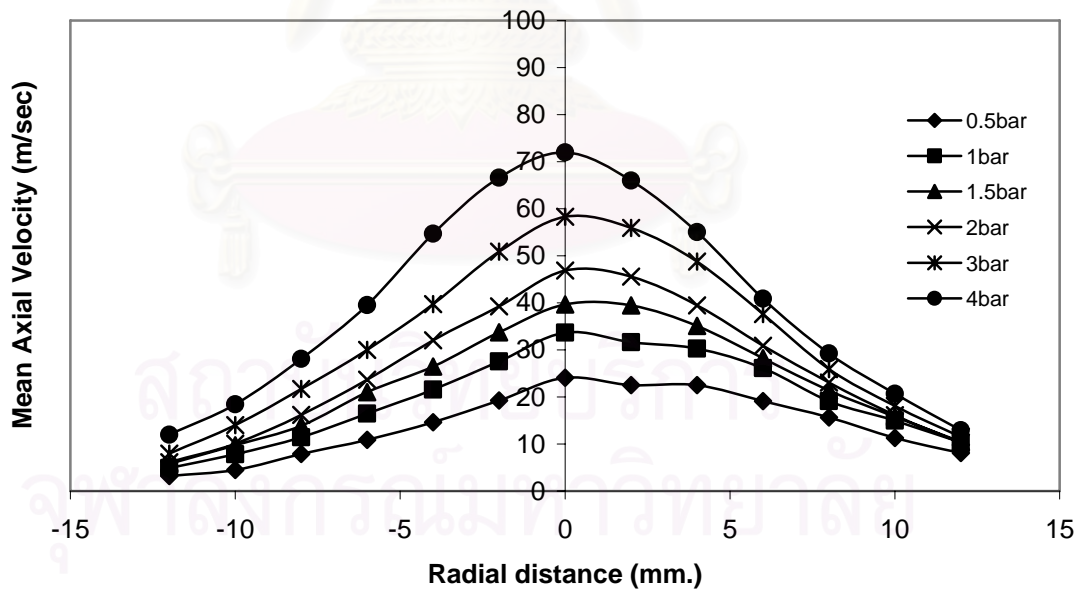


Figure 6.21 Axial mean velocity of PO20:D80 with different injection pressure at 7 cm. away from atomizer tip

Finally, it can be concluded from Table 6.4 that the mean velocity of drops depends only on air injection pressure.

Table 6.4 Axial mean velocities of fuel droplets at the center of the spray

Traveling distance (cm)	Air injection pressure (bar)	Axial mean velocity (m/sec)
5	0.5	35
	1	50
	1.5	60
	2	70
	3	80
	4	90
7	0.5	23
	1	34
	1.5	40
	2	48
	3	59
	4	71

CHAPTER 7

CONCLUSIONS AND RECOMMENDATIONS

7.1 Concluding Remarks

The aim of this research was to characterize the spray from the two-fluid atomizer with diesel blended with palm oil. The study of the characteristics of the spray such as drop size and velocity were conducted by a PDA. The homemade PDA was also studied to gain optic knowledge. It can be concluded that the homemade PDA in CEPT is successfully working for velocity measurement with some error which depended on alignment and optic parameters. The following conclusions were made according to the experimental measurement using the commercial PDA.

- 1) Most of the spray is air which can be seen from the discharge coefficient which was quite low (0.05-0.1) along increasing of injection pressure. However, increasing of viscosity caused a decrease of the discharge coefficient which meant more viscous liquid can be difficult to atomize.
- 2) At low air injection pressure (0.5-1 bars) large drops are generated (30-20 micron) with regards to SMD. The velocity of drops is significantly higher when atomizing air is increased.
- 3) The two-fluid spray drops are not stable along traveling distance; the larger drops and lower velocity are found at longer downstream distance.
- 4) The drop size distribution is symmetric around radial distance. The large drops are found in the center of the spray but the larger drops are also found at the outskirts in some experiments. Likewise, the highest droplet velocity is found at the center region.
- 5) The fuel properties such as viscosity, density, and surface tension affected the size distribution. Especially, viscosity caused poor atomization. However, the fuel properties did not affect the velocity profile because the air injection pressure has more effect on velocity. The injection pressure

around 0.5 to 4 bars produced the different drop axial mean velocity around 30 to 90 m/sec.

7.2 Recommendations

7.2.1 Homemade PDA

It does work for velocity measurement but can only be used safely for inflammable liquids. It would be better to change the experimental room into one that has a circulation system. Moreover, it can be well aligned on an optic table. Also, changing some small equipment like cables and optic probes can decrease noise which means the diameter of drops could be measured correctly.

7.2.1 Spray measurement

Possible future research topics that can be studied are:

- 1) Changing liquid fuel, for example, biodiesel or some other type of vegetable oils.
- 2) Changing the atomizer which is used in other applications, for instance, a swirl injector in burner.

Furthermore, it is recommended that the future study should investigate more characteristics of this type of atomizer like the drop break-up to deeply understand the generation of spray which will matter in further study of atomization.

REFERENCES

- [1] Altin, R., Cetinkaya, S., and Yucesu. H.S. (2001). The Potential of using vegetable oil fuels as fuel for diesel engines. *Energy Conversion and Management* 42: 529-538.
- [2] Canakci, M., Erdil, A., and Arcaklioglu, E. (2005). Performance and exhaust emissions of a biodiesel engine. *Applied Energy* 83(6): 594-605.
- [3] Bachalo, W.D., Houser, M.J., and Smith, J.N. (1987). Behavior of Sprays Produced by Pressure Atomizers as Measured Using a Phase/Doppler Instrument. *Atomisation and Spray Technology* 3: 53-72.
- [4] Shaine Tyson, K. (1992). *Biodiesel Handling and Use Guidelines*. U.S. Department of Energy.
- [5] Machacon, H.T.C., Matsumoto, Y., Ohkawara, C., Shiga, S., Karasawa, T., and Nakamura, H. (2001). The effect of coconut oil and diesel fuel blends on diesel engine performance and exhaust emissions. *Society of Automotive Engineers of Japan* 22: 349-355.
- [6] Silvio C.A. de Almeida, Belchior, C.R., Nascimento, M.V.G., Leonardo dos S.R. Vieira, and Fleury, G. (2002). Performance of a diesel generator fuelled with palm oil. *Fuel* 81: 2097-2102.
- [7] Ramadhas, A.S., Jayaraj, S., and Muraleedharan, C. (2005). Characterization and effect of using rubber seed oil as fuel in the compression ignition engines. *Renewable Energy* 30: 795-803.
- [8] Ramesh, N.R., Sridhara, K., and Natarajan, R. (1985). Studies on the atomization and combustion performance of a twin-fluid acoustic atomizer. *Fuel* 64(12): 1677-1680.
- [9] Sindayihebura, D., and Dumouchel, C. (1999). Low-frequency ultrasonic atomization of large liquid flow rates. Proceedings of the 15th edition of ILASS Europe Conferences, Toulouse, France.

- [10] Ejim, C.E., Fleck, B.A., and Amirfazli, A. (2005). A scaling Study of the Atomization of a Two-Phase Industrial Nozzle: Part1 – Effect of Surface Tension and Viscosity on Mean Drop Size Profiles. *Proceeding of the 19th Annual Conference on Liquid Atomization and Spray Systems*, Olean, France: 367-372.
- [11] Boonnathee, T. (2004). *Development of phase Doppler anemometer for measuring velocity and size distribution of water droplets*. Master's Thesis, Department of Chemical Engineering, Faculty of Engineering, Chulalongkorn University.
- [12] Bachalo, W.D. (1980). Method for measuring the size and velocity of spheres by dual-beam light-scatter interferometry. *Applied Optics* 19(3): 363-370.
- [13] Yule, A.J., and Filipovic, I. (1992). On the break-up times and lengths of diesel sprays. *International Journal of Heat and Fluid Flow* 13(2): 197-206.
- [14] Ramadhas, A.S., Jayaraj, S., and Muraleedharan, C. (2004). Use of vegetable oils as I.C. engine fuels-A review. *Renewable Energy* 29: 727-742.
- [15] Anwar, F., Hussain, A.I., Iqbal, S., and Bhangar, M.I. (2006). Enhancement of the oxidative stability of some vegetable oils by blending with Moringa oleifera oil. *Food Chemistry* 103(4): 1181-1191.
- [16] Lichtarowicz, A., Duggins, R.K., and Markland, E. (1965). Discharge coefficient for incompressible non-cavitating flow through long orifices. *Journal of Mechanical Engineering Science*, 7(2), 210-219. Cited in Lefebvre, A.H. (1989). *Atomization and Sprays*. London: Hemisphere Publishing Corporation.
- [17] Lefebvre, A.H. (1989). *Atomization and Sprays*. London: Hemisphere Publishing Corporation.
- [18] Williams, A. (1990). *Combustion of Liquid Fuel Sprays*. London: Butterworths&Co.
- [19] Crowe, C., Sommerfeld, M., and Tsuji, Y. (1992). *Multiphase Flows with Droplets and Particles*. London: CRC Press.

- [20] Dantec Ltd. *Dantec dynamics measurement technology*. Available from : <http://www.dantecdynamics.com>, [2005, November]
- [21] Rizk, N.K., and Lefebvre, A.H. (1984). Influence of downstream distance on simplex atomizer spray characteristics. *The American Society of Mechanical Engineers*.
- [22] Lefebvre, A.H. (1980). Airblast Atomization. *Progress in Energy and Combustion Science* 6: 233-261.
- [23] Chin, J.S., Nickolaus, D., and Lefebvre, A.H. (1986). Influence of downstream distance on the spray characteristics of pressure-swirl atomizers. *Journal of Engineering for Gas Turbines and Power* 108: 219-224.
- [24] Chen, Y.C., Starner, S.H., and Marsi, A.R. (2006). A detailed experimental investigation of well-defined, turbulent evaporating spray jets of acetone. *International Journal of Multiphase Flow* 32: 389-412.
- [25] Kufferath, A., Wende, B., and Leuckel, W. (1999). Influence of liquid flow conditions on spray characteristics of internal-mixing twin-fluid atomizers. *International Journal of Heat and Fluid Flow* 20: 513-519.
- [26] Drain, L.E. (1980). *The Laser Doppler Technique*. New York: John Willy & Sons Ltd.
- [27] Nwafor, O.M.I., and Rice, G. (1996). Performance of Rapeseed Oil Blends in a Diesel Engine. *Applied Energy* 54: 345-354.
- [28] Black, D.L., McQuay, M.Q., and Bonin, M.P. (1996). Laser-based techniques for particles-size measurement: A review of sizing methods and their industrial applications. *Prog. Energy Combust. Sci* 22: 267-306.
- [29] Yule, A.J., Ereaut, P.R., and Ungut, A. (1983). Droplet sizes and velocities in Vaporizing sprays. *Combustion And Flame* 54: 15-22.



APPENDICES

สถาบันวิทยบริการ
จุฬาลงกรณ์มหาวิทยาลัย



APPENDIX A
BASIC OPTICS

สถาบันวิทยบริการ
จุฬาลงกรณ์มหาวิทยาลัย

The basic knowledge of optics can be found in any standard optical textbook. This section is based on “The Laser Doppler Technique.” written by Drain L.E. [26].

A.1 Light as Electromagnetic Radiation

Light is a special case of the general type of radiation arising from the interaction of electric and magnetic fields. The spectrum of electromagnetic waves extends from long radio waves to the r -rays of nuclear physics and all these waves travel with the same velocity, i.e. $C_0 = 2.99776 \times 10^8 \text{ m s}^{-1}$. The range of wavelengths or frequencies is conventionally divided into regions depending on the common methods of production and detection. The main divisions are shown in Figure A.1. Visible radiation has wavelengths in the range approximately $0.40 - 0.70 \mu\text{m}$, depending on the color.

The technique of velocity and size measurement by means of the Doppler shift is applied to the whole range of electromagnetic waves but the practical methods discussed in this work apply principally to wavelengths of around the visible region. The neighboring ultra-violet and infrared regions may also be included and these waves may be loosely referred to as light.



สถาบันวิทยบริการ
จุฬาลงกรณ์มหาวิทยาลัย

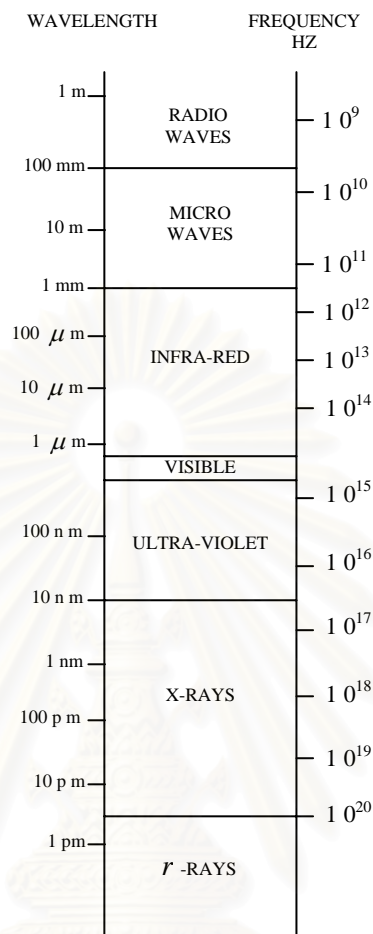


Figure A.1 The electromagnetic spectrum. [26]

A.2 Geometrical Optics

In many situations, the use of elementary geometrical optics is all that is needed to determine the propagation of light beams and much of the design of LDA and PDA systems is based on these principles. In this approximation the laws are as follows:

- (i) in a uniform medium light travels in straight lines along rays
- (ii) when rays are reflected at a smooth surface, the angle of incidence is equal to the angle of reflection

- (iii) when passing from one medium to another, light is deviated or refracted, the angles of incidence and refraction θ_1 and θ_2 (see Figure A.2) being related by Snell's law

$$\frac{\sin \theta_1}{\sin \theta_2} = \frac{n_2}{n_1} \quad (\text{A.1})$$

where n_1 and n_2 are the refractive indices of the media (usually referred to vacuum) for the particular wavelength used.

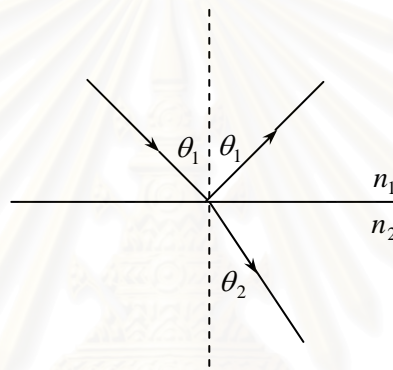


Figure A.2 Reflection and refraction of light at a plane surface.

Refraction from a dense to a less dense medium ($n_2 < n_1$) is not possible if $\theta_1 > \sin^{-1}(n_2/n_1)$. In this case the incident light is totally reflected. Total internal reflection inside prisms is often used for beam deflection.

The most familiar optical devices using the principle of refraction are lenses. They have many uses in a PDA system for example expanding and focusing laser beams, image formation, and concentrating light onto detectors. The lens performance required is usually less demanding than in most optical instruments or in photography, and for most PDA applications simple one-component lenses are adequate. This is because of the small diameters of laser beams and monochromatic nature of the light.

A.3 Interference

The wave nature of light is very evident in the phenomenon of interference, which occurs when two beams are superimposed. If the light beams have a sufficiently well defined frequency and consistent phase relation, light and dark bands, interference fringes, can be observed. A simple situation of this type, often applied in PDA work, is the crossing of two parallel beams at an angle α . This may be produced for example by splitting a plane wave with a small angle prism (Fresnel biprism), as shown in Figure A.3. Points in the crossover region are subject to the alternating electric fields of both beams. Where these alternations are in phase, the resultant electric field amplitude is the sum of the amplitudes from the two beams, and an increase in light intensity is obtained. Where the alternations are out of phase, the resultant is the difference of the amplitudes, and the light intensity is reduced.

The phases of the electric field alternations produced by the beams at a point P in Figure A.3 are determined by the distances x_1 and x_2 measured along the beams from reference planes. Constructive interference occurs for

$$x_1 - x_2 = n\lambda + \phi \quad (\text{A.2})$$

where λ is the light wavelength, n is an integer and ϕ is a phase constant. Points satisfying this condition lie on planes bisecting the angle between the two beams and separated by a distance s given by

$$s = \frac{\lambda}{2\sin(\alpha/2)} \quad (\text{A.3})$$

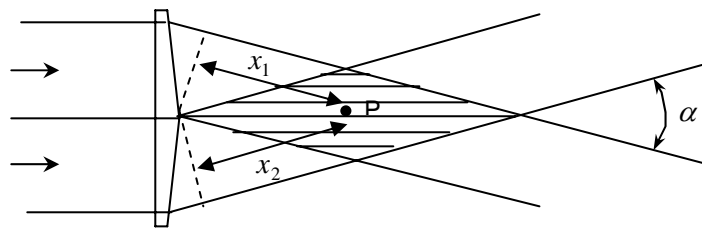


Figure A.3 The formation of interference fringes by parallel light beams crossing at an angle α .

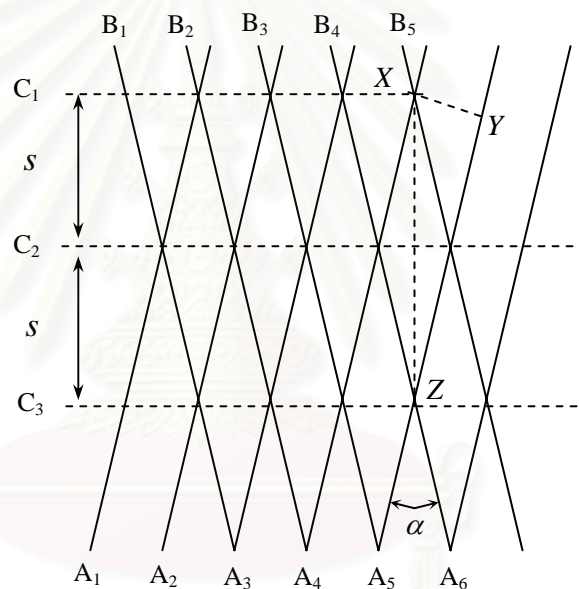


Figure A.4 Diagram showing the relation of interference fringes to the wave fronts of intersecting beams.

Each plane corresponds to a different value of n . This formula may easily be derived by mathematical analysis or by the geometrical construction shown in Figure A.4. Planes of equal phase, wave fronts, separated by one wavelength are drawn for each beam. These are denoted by $A_1, A_2, \dots, B_1, B_2, \dots$, etc. and could be interpreted as wave crests at a particular instant. The points where the waves reinforce lie on the planes C_1, C_2 , etc. The separation of these bright fringes is denoted by s .

Consideration of the right-angled triangle XYZ formed by the construction shown immediately yields formula (A.3)

A.4 Diffraction

A consequence of the wave nature of light is the derivation from the strict straight-line law of propagation assumed in geometrical optics. A beam only travels in a straight line if its diameter is very large compared with the wavelength λ . The divergence of a beam of diameter d is given approximately by λ/d . Diffraction sets a limit to the definition and resolution obtainable in an optical system. Optical systems giving as good a definition as is theoretically possible are termed diffraction limited.

Most problems with the diffraction of light may be solved by the application of Huygens's principle, an old idea but still a valid approach. It may be derived as an approximation from electromagnetic theory. This principle enables the optical field to be derived from a given wave front by treating infinitesimal elements of the wave front as point sources having amplitude proportional to the amplitude of the incident light at that point. The total amplitude at any given point is obtained by integrating the contribution from every point on the wave front.

A.5 Gaussian Beam Optics

In most laser applications it is necessary to focus, modify, or shape the laser beam by using lenses and other optical elements. In general, laser-beam propagation can be approximated by assuming that the laser beam has an ideal Gaussian intensity profile, corresponding to the theoretical TEM_{00} mode. Coherent Gaussian beams have peculiar transformation properties that require special consideration. In order to select the best optics for a particular laser application, it is important to understand the basic properties of Gaussian beams.

In PDA, we are more often concerned with Gaussian intensity distribution. The intensity distribution across the beam is Gaussian in all cross-sections. In general, a 'Gaussian' beam has the shape shown in Figure A.5 [3]. The radius r_z of the beam of $1/e^2$ intensity points at a typical cross-section is given by:

$$r_z^2 = \frac{\lambda^2 z^2}{\pi^2 r_0^2} + r_0^2 \quad (\text{A.4})$$

where z is the distance along the beam from the cross-section of minimum diameter or ‘waist’ and r_0 is the radius at the waist (the distance from the center where the intensity is reduced to $1/e^2$ of its maximum value) in the focal plane. At the waist we have a plane wave but elsewhere the beam is converging or diverging. The angle of divergence or convergence (ϕ) at distance z is

$$\phi = \frac{2 dr_z}{dz} = \frac{2\lambda^2 z}{\pi^2 r_0^2 r_z} = \frac{2\lambda}{\pi r_0} \left/ \left(1 + \frac{\pi^2 r_0^4}{\lambda^2 z^2} \right)^{1/2} \right. \quad (\text{A.5})$$

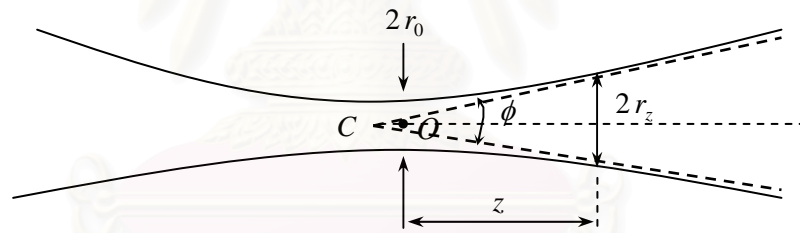


Figure A.5 Characterization of a Gaussian beam [26]

These relations may be used to calculate the propagation of Gaussian beams where diffraction effects are important. For example, we see that a plane wave (which corresponds to the waist position in Figure A.5) spreads out by diffraction to a limiting divergence angle ϕ_∞ at infinity of

$$\phi_\infty = \frac{2\lambda}{\pi r_0} \quad (\text{A.6})$$

It is interesting to note that when a parallel Gaussian beam is focused by a lens, the minimum beam diameter does not occur exactly at the focal plane but

slightly nearer the lens. The difference is sometimes significant for narrow beams and long focal lengths. Supposing that the light is traveling from right to left in Figure A.5, it may be considered the converging beam at the plane z to be formed from a parallel beam by a lens in that plane. The distance of the center of the waist from the point of convergence C may be calculated from equations (A.4) and (A.5) In terms of the focal length F and the radius of the beam at the lens R_0 we have:

$$OC = F - z = F / \left(1 + \frac{\pi^2 R_0^4}{\lambda^2 F^2} \right) \quad (\text{A.7})$$

or approximately

$$F \left(\frac{F\lambda}{\pi R_0^2} \right) \quad (\text{A.8})$$

when $R_0^2 \gg F\lambda$

A.6 Polarization of Light Waves

In electromagnetic radiation, the oscillating field is transverse to the direction of propagation. This allows a degree of freedom for the orientation of the field or different states of polarization. The plane containing the electric field and the direction of propagation will be called the ‘plane of polarization’, but the convention on this is not universal.

Figure A.6 shows that the electric and magnetic vectors associated with an electromagnetic wave are at right angles to each other and also to the direction of wave propagation is firm evidence of the transverse nature of electromagnetic waves.

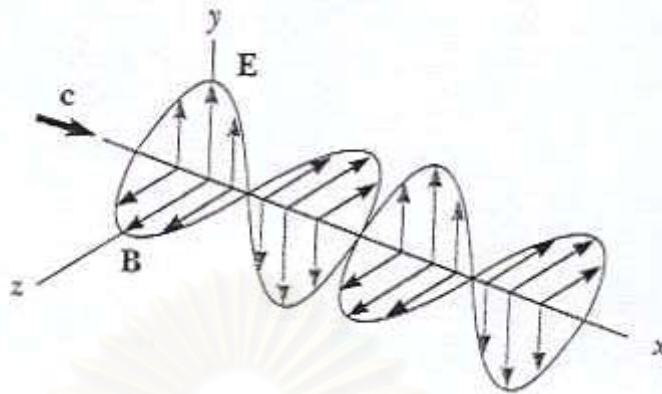


Figure A.6 Schematic diagram of an electromagnetic wave propagating in the x direction. The electric field vector E vibrates in the xy plane, and the magnetic field vector B vibrates in the xz plane.

An ordinary beam of light consists of a large number of waves emitted by the atoms or molecules of the light source. Each atom produces a wave with its own orientation of E , as in Figure A.6, corresponding to the direction of atomic vibration. The direction of polarization of the electromagnetic wave is defined to be the direction in which E is vibrating. However, because all directions of vibration are possible, the resultant electromagnetic wave is a superposition of waves produced by the individual atomic sources. The result is an unpolarized light wave, described in Figure A.7 (a). The direction of wave propagation in this figure is perpendicular to the page. Note that all directions of the electric field vector, lying in a plane perpendicular to the direction of propagation, are equally probable. At any given point and at some instant of time, there is only one resultant electric field.

A wave is said to be linearly polarized if E vibrates in the same direction at all times at a particular point, as in Figure A.7 (b). The wave described in Figure A.6 is an example of a wave linearly polarized in the y direction. As the wave propagates in the x direction, E is always in the y direction. The plane formed by E and the direction of propagation is called the plane of polarization of the wave.

In Figure A.6 the plane of polarization is the xy plane. It is possible to obtain a linearly polarized beam from an unpolarized beam by removing all waves from the beam except those whose electric field vectors oscillate in a single plane.

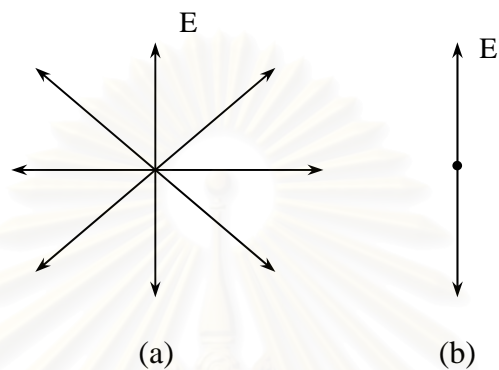


Figure A.7 (a) An unpolarized light beam viewed along the direction of propagation (perpendicular to the page). The transverse electric field vector can vibrate in any direction with equal probability. (b) A linearly polarized light beam with the electric field vector vibrating in the vertical direction.

สถาบันวิทยบริการ
จุฬาลงกรณ์มหาวิทยาลัย



APPENDIX B
CONFERENCE PAPERS

สถาบันวิทยบริการ
จุฬาลงกรณ์มหาวิทยาลัย

APPENDIX B1
CHARACTERISTICS OF BIODIESEL OIL ATOMIZED
BY A TWO-FLUID NOZZLE USING PDA

13TH REGION SYMPOSIUM ON CHEMICAL
ENGINEERING, RSCE 2006, SINGAPORE, DEC 3-5.



สถาบันวิทยบริการ
จุฬาลงกรณ์มหาวิทยาลัย

Characteristics of Biodiesel Oil Atomized by a Two-Fluid Nozzle Using PDA

Juthamas Kamrak^a, Tawatchai Charinpanitkul^a, Gerard Grehan^b

^a Center of Excellence in Particle Technology, Faculty of Engineering, Chulalongkorn University, Bangkok, Thailand, juthamas_kamrak@yahoo.com

^b LESP/UMR CNRS6614/ INSA et Université de Rouen , BP 12, avenue de l'université , 76801, Saint Etienne du Rouvray, France

ABSTRACT

Drop size and velocity distribution in a spray of fuel play an important role in determining combustion efficiency. The Phase Doppler anemometer (PDA) is a well-established technique allowing simultaneous measurement of velocity and size of droplets. In this work, effect of bio-substitute component on the size and velocity of biodiesel droplets which are generated by a two-fluid nozzle are investigated comprehensively using a PDA.

1. INTRODUCTION

Due to the energy crisis, a skyrocketing increase in fuel prices arouses many scientists and researchers to pay more attention to alternative fuel sources. Among them, the study of vegetable oil utilization becomes of interest due to the abundance and renewability of this source [1]. Vegetable oils can be directly mixed with diesel oil as a substitute component. It has been proved experimentally that the use of vegetable oils in engines is applicable with some minor system modifications [2].

To gain an insight into the efficient combustion of those fuels, the detailed measurements of fuel spray drop size and velocity distributions are crucial. The essential data must include simultaneous drop size and velocity measurements at certain locations [3]. In general, those data could be used to design the combustion chamber in the engine or furnace. To date, there have been many techniques such as imaging or techniques with hybrid light scatter detection systems combined with the Laser Doppler Velocimeter (LDV).

2. EXPERIMENTS

The mixture of palm oil and diesel is used as fuel in this study. First, twenty percent by volume of palm oil is taken into account because it is the most promising mixture ratio to be actually employed. The properties of pure diesel and biodiesel are shown in table 1.

Table 1 The fuels properties

	Density (kg/m ³)	Kinematic Viscosity (mm ² /s)	Surface Tension (mN/m)	Refractive index
Diesel	832.20	3.23±0.00	28.00±0.00	1.466
B20	850.18	5.26±0.00	28.78±0.15	1.467

Drop size and velocity measurement are carried out at various positions below the tip of the nozzle. The axial distribution of spray characteristics were studied at 5 and 7 cm measured downstream from the nozzle tip. At each position measurements along radial direction were conducted by using a step size of 2mm. The injection pressures for atomization are varied in a range of 0.5, 1, 1.5, 2, 3 and 4 bar.

The sprays produced by the two-fluid nozzle were analyzed by the PDA. The system consists of two parts, an emitting and a collecting part. The laser beams from the first part are crossed at the intersection point which is called measurement volume. The scattered lights are collected by the second part and they contain the drop size and velocity information.

3. RESULTS AND DISCUSSION

3.1 Mean Drop Diameter

Typical examples of the drop size distribution are presented in Fig 1 and Fig 2. The average mean diameter (D_{10}) at 5 and 7 cm downstream from the atomizer tip are plotted

against the radial position. The largest droplets preferably appear at the center of the spray. A gradual decrease in drop size could be observed when injection pressure was increased. It should be noted that within the investigating conditions traveling distance exerts some slight influence on the drop size distribution.

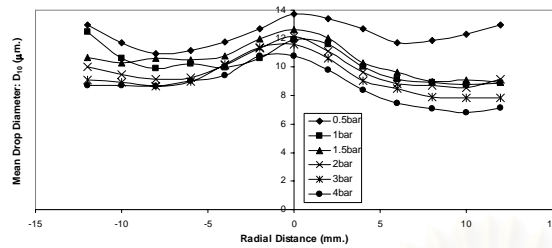


Fig. 1 Mean drop diameter distribution at 5 cm downstream from nozzle

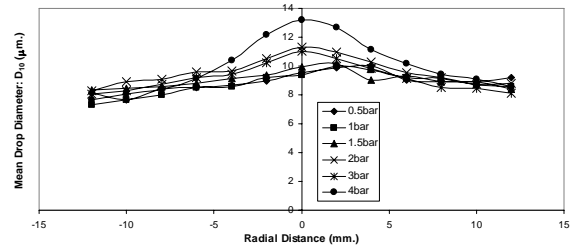


Fig. 2 Mean drop diameter distribution at 7 cm downstream from nozzle

3.2 Mean drop velocities

Figure 3 and 4 exhibit the radial distribution of the axial average droplet velocities. It can be clearly seen that the radial distribution of the droplet velocity is a function of the injection pressure. Without external disturbance, atomized droplets could travel with axial velocity, which are normally distributed over the radial distance.

The longer the traveling distance, the higher the kinetic energy dissipated, therefore more remarkable effects of the traveling distance on the droplet velocity distribution could be expected.

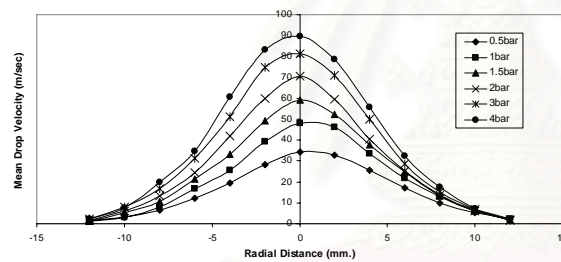


Fig. 3 Mean drop velocity distribution at 5 cm downstream from nozzle

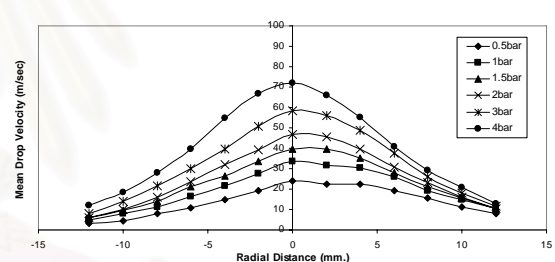


Fig. 4 Mean drop velocity distribution at 7 cm downstream from nozzle

CONCLUSION

In this study, a two-fluid atomizer was employed to atomize droplets of biodiesel, and analyses by a PDA were conducted accordingly. An increasing injection pressure provides a significant effect on drop velocity but a trivial influence on drop size. At the center of the spray, the highest drop velocity and size are observed by the PDA.

REFERENCE

- [1] Altin, R., Cetinkaya, S., and Yucesu. H.S. (2001). *The Potential of using vegetable oil fuels as fuel for diesel engines*. Energy Conversion and Management, 42, 529-538.
- [2] Silvio C.A. de Almeida, Belchior, C.R., Nascimento, M.V.G., Leonardo dos S.R. Vieira, and Fleury, G. (2002). *Performance of a diesel generator fuelled with palm oil*. Fuel, 81, 2097-2102.
- [3] Crowe, C., Sommerfeld, M., and Tsuji, Y. (1992). *Multiphase Flows with Droplets and Particles*. London: CRC Press.

APPENDIX B2
EFFECT OF BIODIESEL OIL COMPOSITION ON
DROPLET SIZE DISTRIBUTION

5TH ASIAN AEROSOL CONFERENCE, AAC 2007,
KAOSHIUNG, TAIWAN, AUG 26-29.



สถาบันวิทยบริการ
จุฬาลงกรณ์มหาวิทยาลัย

Effect of biodiesel oil composition on droplet size distribution

Juthamas Kamrak^{a*}, Patcharaporn Lorturn^a, Gerard Grehan^b, Sawitree Saengkaew^{a,b}
and Tawatchai Charinpanitkul^a

^aCenter of Excellence in Particle Technology, Faculty of Engineering, Chulalongkorn University, Bangkok, Thailand

^bLESP/UMR CNRS6614/ INSA et Université de Rouen , BP 12, avenue de l'université , 76801, Saint Etienne du Rouvray, France

Corresponding author* : Fax: +662 218 6899, email: juthamas_kamrak@yahoo.com

ABSTRACT

Droplet size distribution of biodiesel oil with various compositions was investigated in this work. The droplets generated by a two-fluid atomizer were measured by a commercial PDA. It was found that viscosity of the fuel has a strong effect on the drop size distribution. Additionally, effect of air injection pressures applied to atomize the spray was taken into account. Shear force induced by flow field exerts an effect on distribution of biodiesel droplets in atomized spray.

Keyword: *Drop size distribution, biodiesel, atomization*

1. INTRODUCTION

At present, world energy crisis has aroused researchers to find other alternative fuels. Among those alternatives, biodiesel has gained more attention because of its environmental friendliness and abundance [1]. Also, physical characteristics of such biodiesel are in equivalent level with that of petrodiesel. Therefore, it has been well recognized that biodiesel can be used in many conventional vehicles [2]. Anyway, it has not been clearly understood how composition of the biodiesel will affect its characteristics, in particular for engineering aspects its droplet size distribution which would affect the combustion efficiency [3]. In this work, the effect of biofuel composition on size distribution of droplets generated by a two-fluid nozzle is investigated to collect fundamental information for improving its combustion. The density and surface tension are slightly effect and complex for drop size distribution.

2. EXPERIMENTAL

The simulated biodiesel oil was prepared by manual mixing commercial petrodiesel oil with palm cooking oil. The compositions were varied within a range of 0 to 100 percent by volume. A two-fluid nozzle was selected as atomizing tool due to its advantages of ease in controlling atomizing air pressure and fuel flow rate. Air injection pressure applied to the nozzle was in the range of 0.5-4 bars. Atomized droplet size distribution is investigated using a commercial Phase Doppler Anemometer (Dantec) equipped with Argon laser ($\lambda \sim 488$ nm) source. Effect of flying distance after being atomized was also investigated by setting the measuring volume at the position of 5 and 7 cm apart from the nozzle tip. Also profile of average droplet diameter within the radial direction of the spray was also investigated experimentally.

3. RESULTS AND DISCUSSION

Figure 1(a) depicts the radial profile of the Sauter Mean Diameter (SMD) of biodiesel droplets within the spray atomized at pressure of 1 bar. With an increase in palm oil content, the SMD of droplets became bigger due to the effect of the increasing viscosity. It should be noted that the higher viscosity could result in the larger initial droplet emerging from the atomizing nozzle. Meanwhile, it was also clearly observed that higher convection and shear in the central region of the spray could lead to the smaller average droplet. At the borders of the spray, coalescence of droplets became more enhanced, resulting in much higher droplet SMD.

As shown in Fig 1(b), an increase in the air injection pressure applied to the nozzle could clearly affect the SMD of the B5 and B20 biodiesel droplets. With the lowest injection pressure of 0.5 bar SMD of the B20 biodiesel was about 30 μm . However, with further increase in the air injection pressure up to 4 bar, only a slight increase in the atomized droplets could be obtained due to the dominating influence of its surface tension [2].

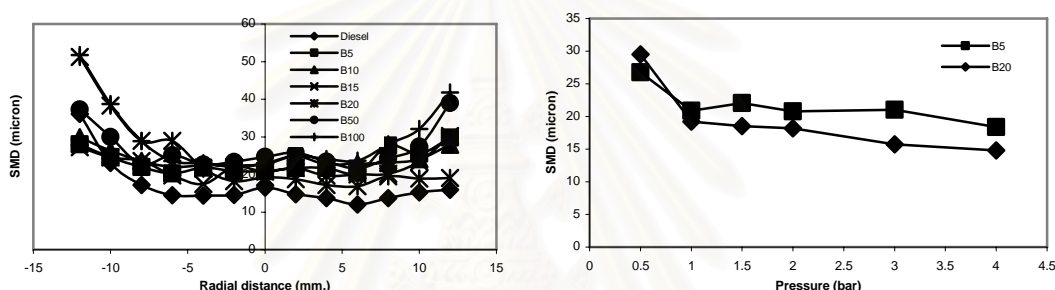


Fig. 1 Effect of biodiesel composition on (a) profile of Sauter Mean Diameter of biodiesel droplets atomized with air injection pressure of 1 bar
(b) Sauter Mean Diameter of B5 and B20 measured at the central part of the spray

4. CONCLUSION

The effect of biodiesel composition was investigated experimentally using a commercial PDA. The increasing viscosity of the biodiesel due to higher fraction of blended palm oil could result in bigger average droplet size. On the other hand, the increasing injection pressure of atomizing air applied to the nozzle could provide higher shear which in turn led to the smaller average droplet diameter.

ACKNOWLEDGEMENT

The authors greatly acknowledge financial support of Silver Jubilee Endowment Fund of Chulalongkorn University and Franco-Thai Collaborative project, as well as partial support of Complexe de Recherche Interprofessionnel en Aerothemochimie (CORIA), France.

REFERENCES

- [1] Tyson, K.S. (1992). *Biodiesel Handling and Use Guidelines*. U.S. Department of Energy.
- [2] Altin, R., Cetinkaya, S., and Yucesu. H.S. (2001). *The Potential of using vegetable oil fuels as fuel for diesel engines*. Energy Conversion and Management, 42, 529-538.
- [3] Lefebvre, A.H. (1989). *Atomization and Sprays*. London: Hemisphere Publishing Corporation.

VITA

Miss Juthamas Kamrak was born on August 30, 1983. In March 2006, she received her Bachelor Degree of Science with specialty 2nd class honor in Chemical Technology from Faculty of Science, Chulalongkorn University, Bangkok, Thailand. Then, she continued her study in Chemical Engineering at Chulalongkorn University. She also got the scholarship from Franco-Thai collaborative for doing her study in Complexe de Recherche Interprofessionnel en Aerothemochimie (CORIA), Rouen, France, for 8 months.



สถาบันวิทยบริการ
จุฬาลงกรณ์มหาวิทยาลัย